

Small x physics: from HERA, through LHC to EIC

Anna Staśto
Penn State University

Outline

Lecture 1

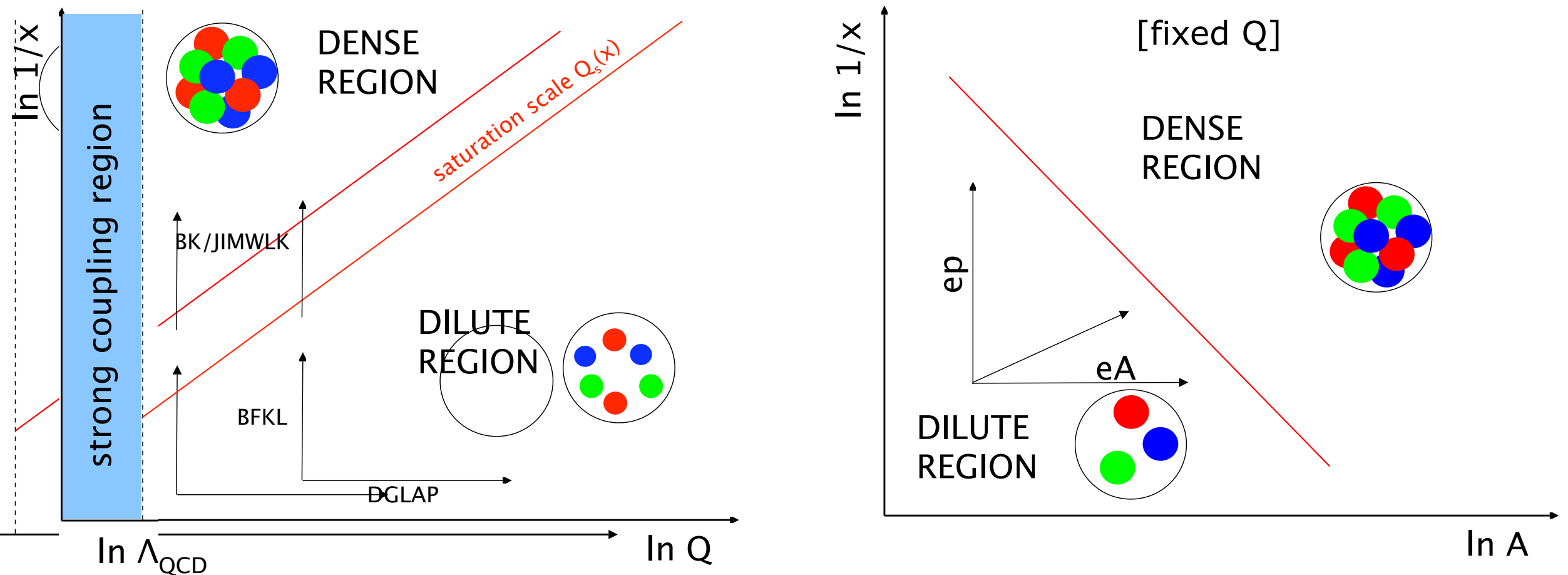
- DIS paradigm: collinear factorization and DGLAP evolution
- Why small x ? A bit of Pomeron history
- BFKL evolution at small x
- NLL BFKL and the problems with convergence
- Collinear resummation at small x
- Parton saturation
- Nonlinear evolution equation. Saturation scale
- Impact parameter dependence(*)

Outline

Lecture 2

- Is BFKL needed ? DGLAP success
- Hints of small x physics in the structure function data
- Two-scales processes
 - Forward jet in DIS
 - $\gamma^*\gamma^*$ at LEP
 - Mueller-Navelet jets at LHC
- Angular correlations of dihadrons/dijets
- Diffraction at small x and nuclei

DGLAP vs BFKL vs nonlinear evolution



Saturation scale: divides dilute and dense regimes. Enhanced in nuclei

$$Q_s^2 \sim Q_0^2 x^{-\lambda} A^{1/3}$$

Opportunities at the EIC to test saturation using nuclei

Capabilities of EIC

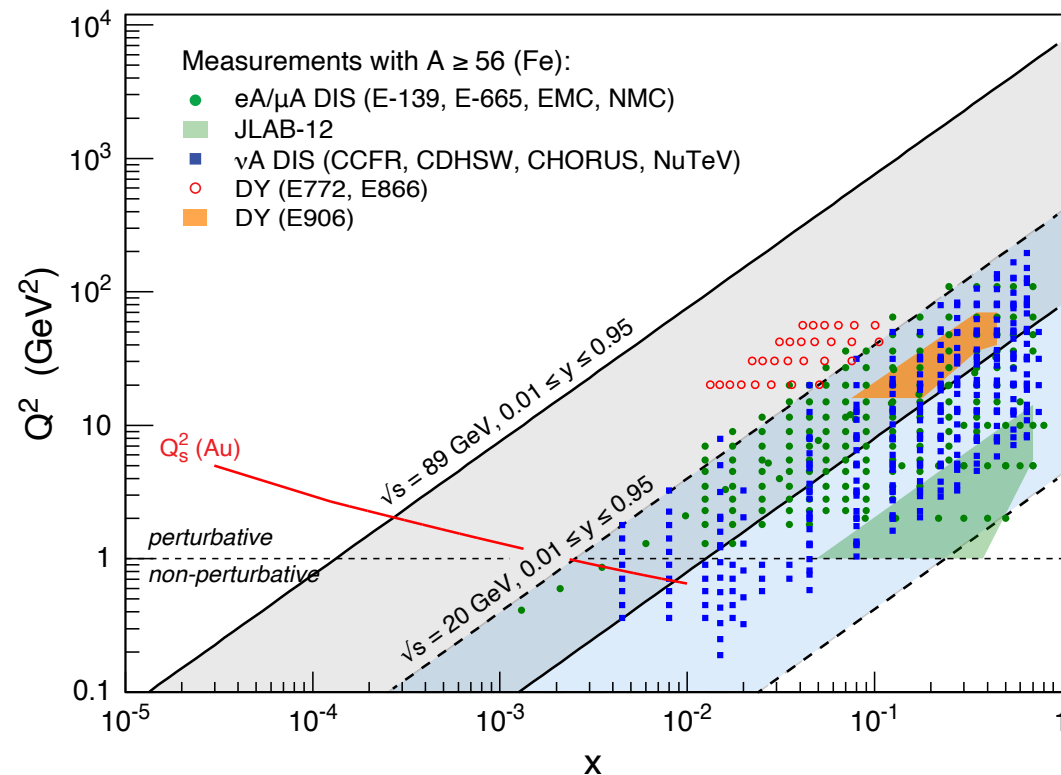
Beams with different A: from *light nuclei* to the *heavy nuclei*

Polarized electron and nucleon beams. Possibility of polarized light ions.

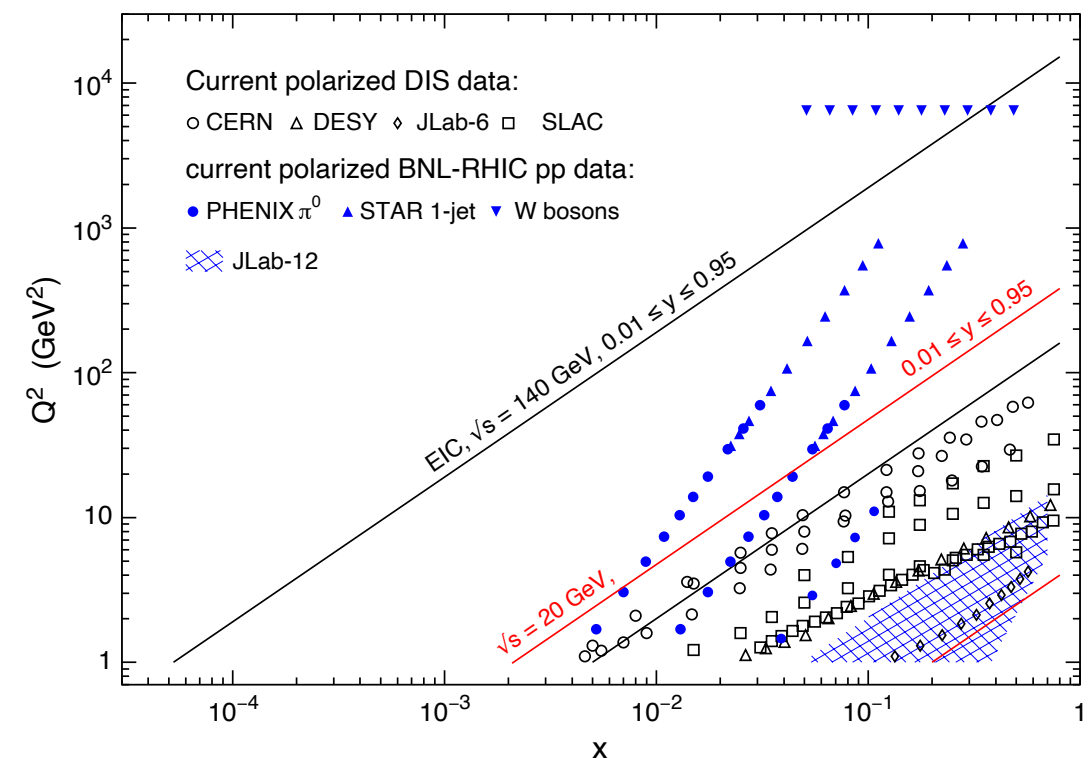
Variable center of mass energies 20 -140 GeV

High luminosity $10^{33} - 10^{34} \text{cm}^{-2} \text{s}^{-1}$

EIC kinematics compared with eA DIS experiments



EIC ep kinematics compared with polarized DIS and pp experiments



What can we learn at EIC at small x and in nuclei?

- **Nuclear structure functions**, precision extraction of nuclear PDFs, testing the **limits** of **collinear factorization** in nuclei. Initial conditions for hot QCD.
- Explore the onset of **saturation** in **eA**, DGLAP vs non-linear evolution, x, A , and Q dependence. Precise measurement of F_L needed (variable energies)
- Extraction of **diffractive nuclear PDFs** possible for the first time, potential for F_L^D . Prospects for measuring Reggeon. **Diffractive to inclusive ratios** needed to distinguish between the different scenarios (saturation vs leading twist shadowing).
- **Exclusive** diffraction of vector mesons, excellent process to **map spatial distribution** and test **saturation**. Experimental challenges.

Successful description of HERA data

Reduced cross section at HERA

Combined measurement H1 and ZEUS

Function of Q^2 for fixed x

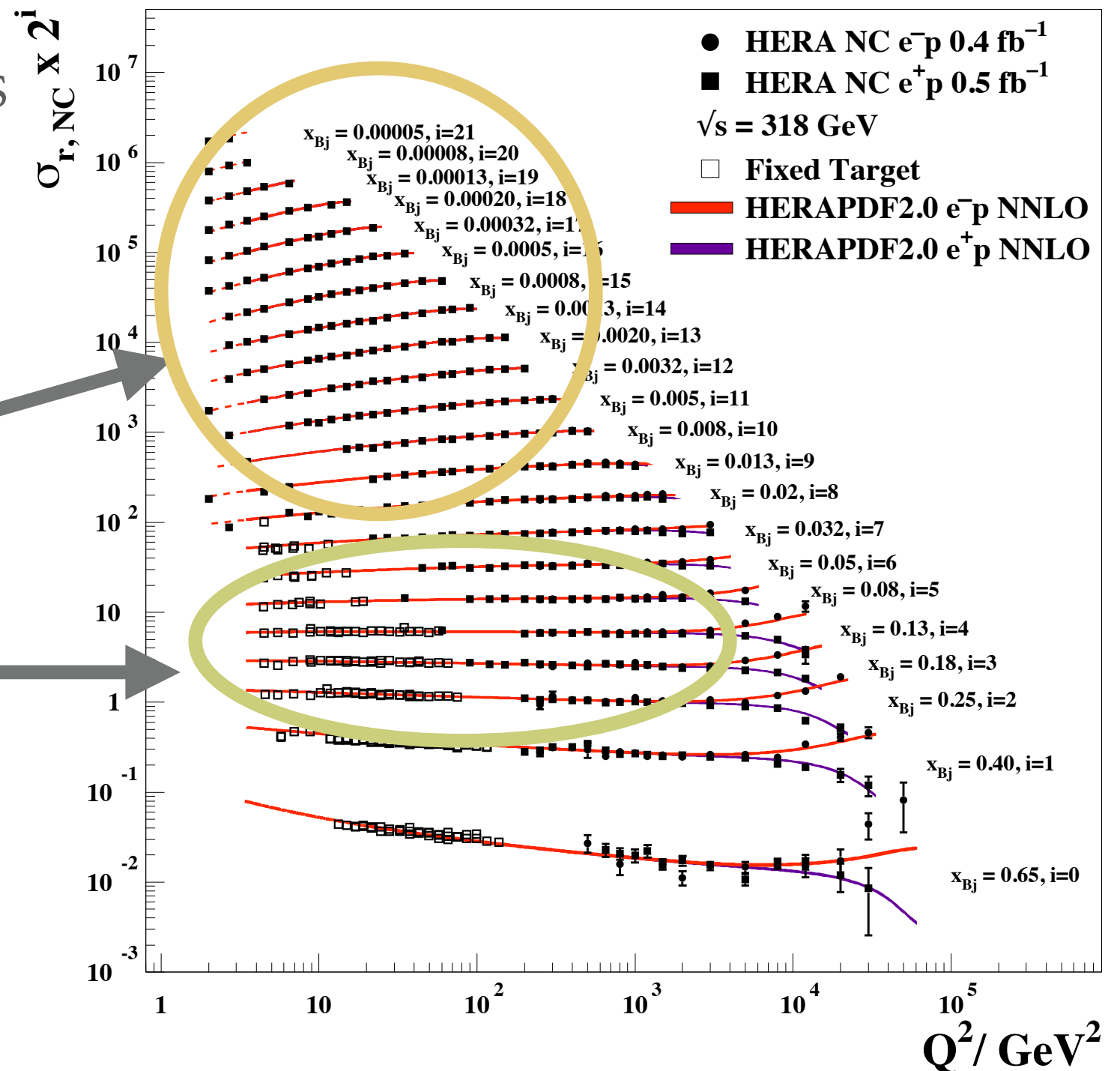
Scaling violations

Scaling region : independent of Q^2

Excellent description using DGLAP

HERAPDF parton densities

H1 and ZEUS

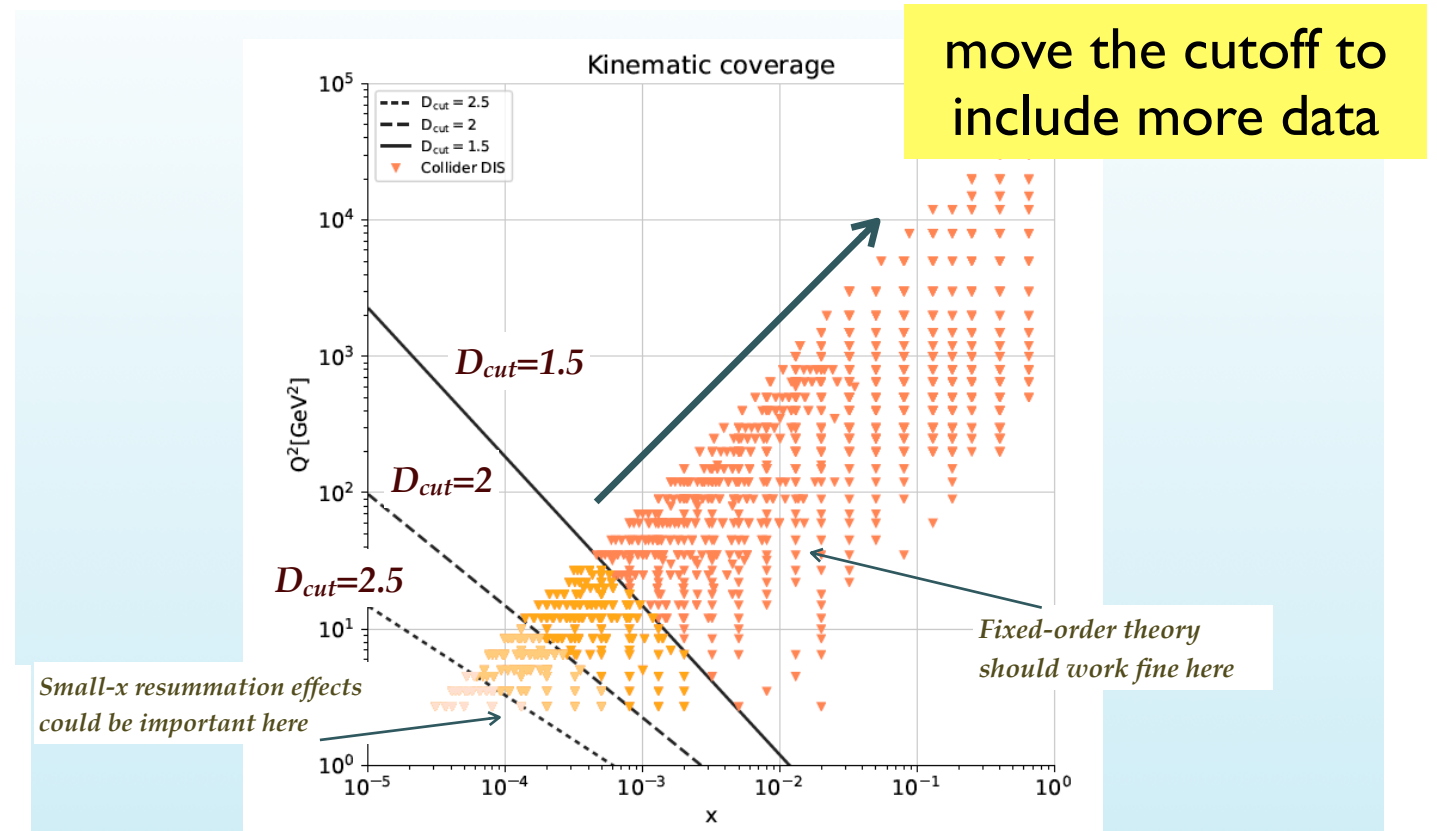
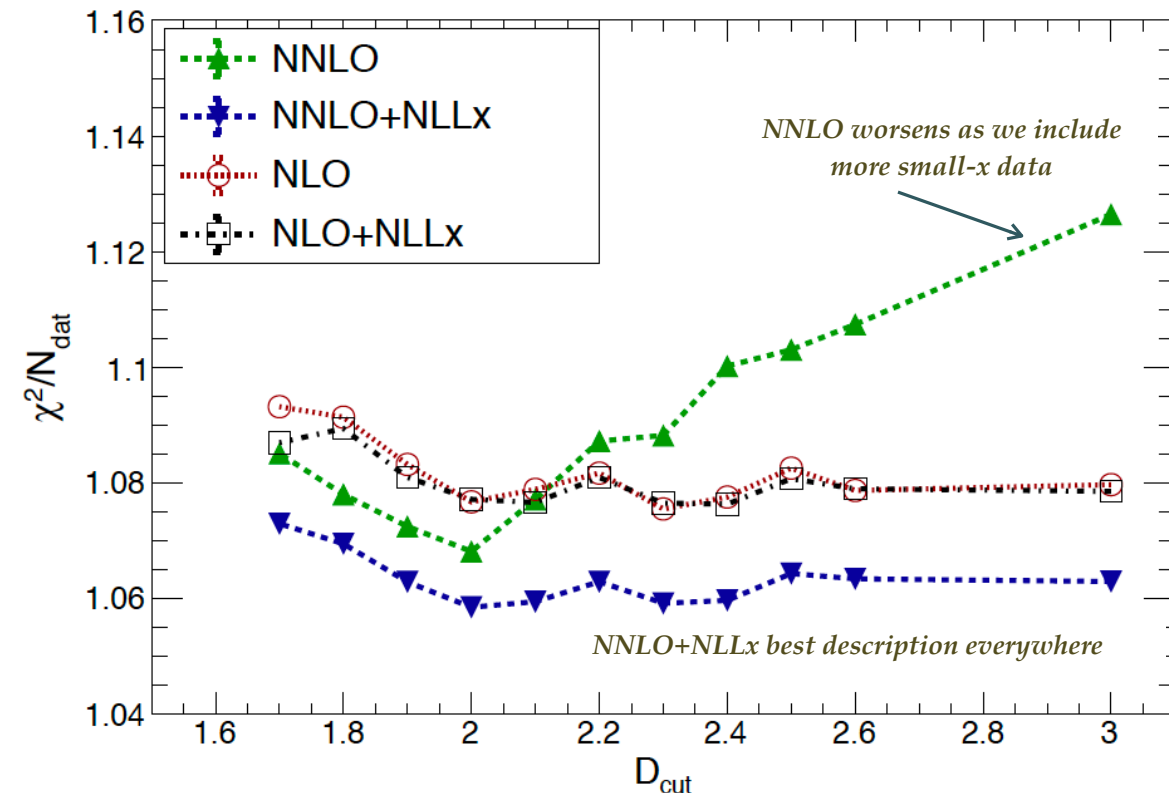


Small x resummation and the HERA data

Ball, Bertoni, Bonvini, Marzani, Rojo, Rottoli

- Perform fits to data with the cut on small x /small Q^2 region
- Observe the variation or lack of variation in χ^2

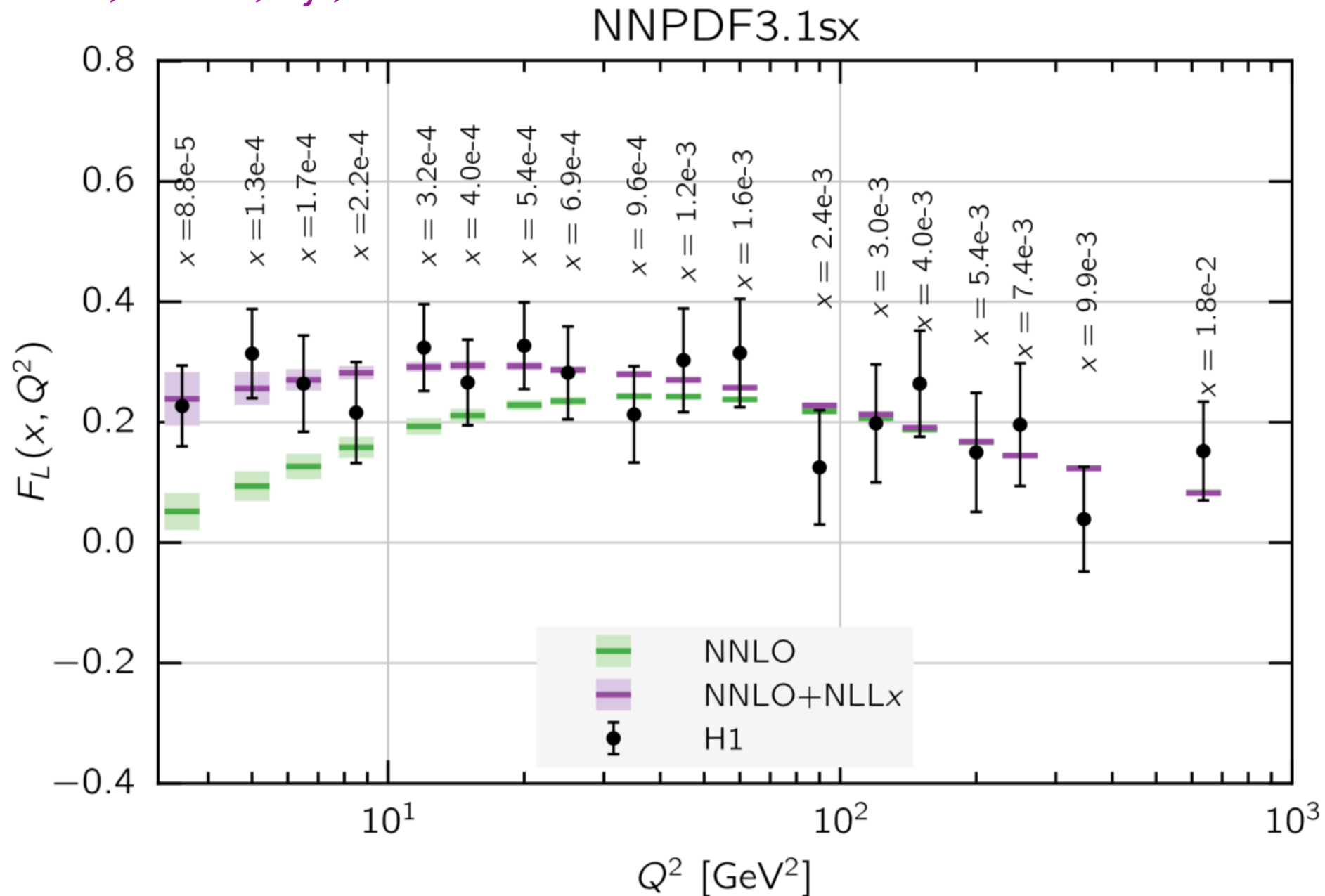
NNPDF3.1sx, HERA NC inclusive data



- χ^2 changes for DGLAP at NNLO when more small x data are included
- NNLO+NNLLx gives best description
- Interestingly NLO and NLO+NLLx do not differ by a lot

Improved description of F_L

Ball, Bertoni, Bonvini, Marzani, Rojo, Rottoli

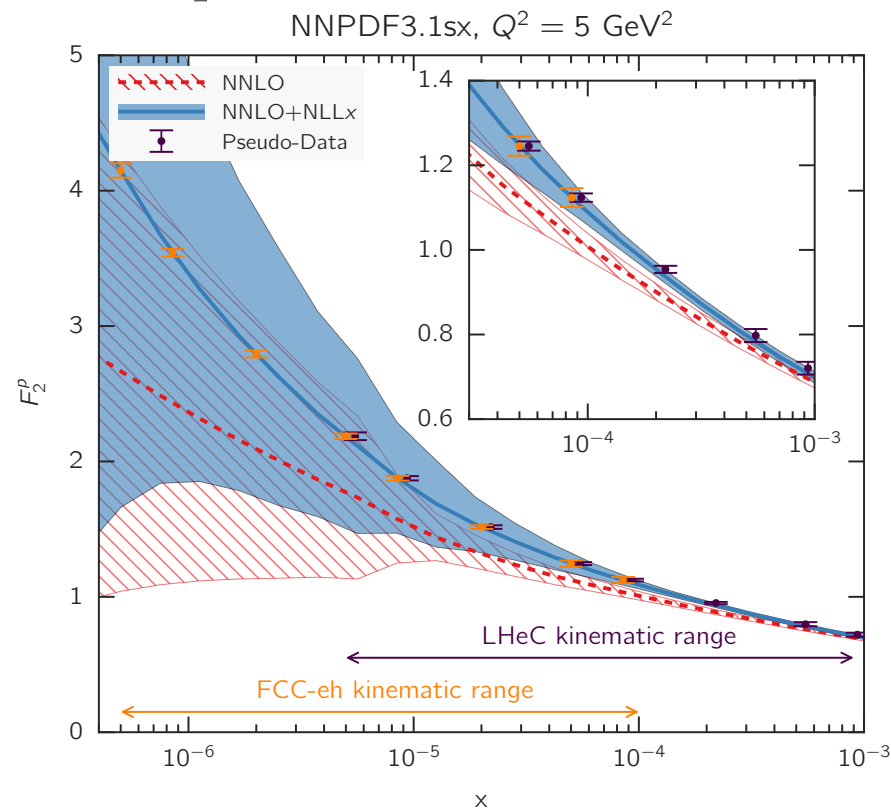


Resummation improves the description of longitudinal structure function at small x

Small x resummation: future DIS facilities

Ball, Bertone, Bonvini,
Marzani, Rojo, Rottoli

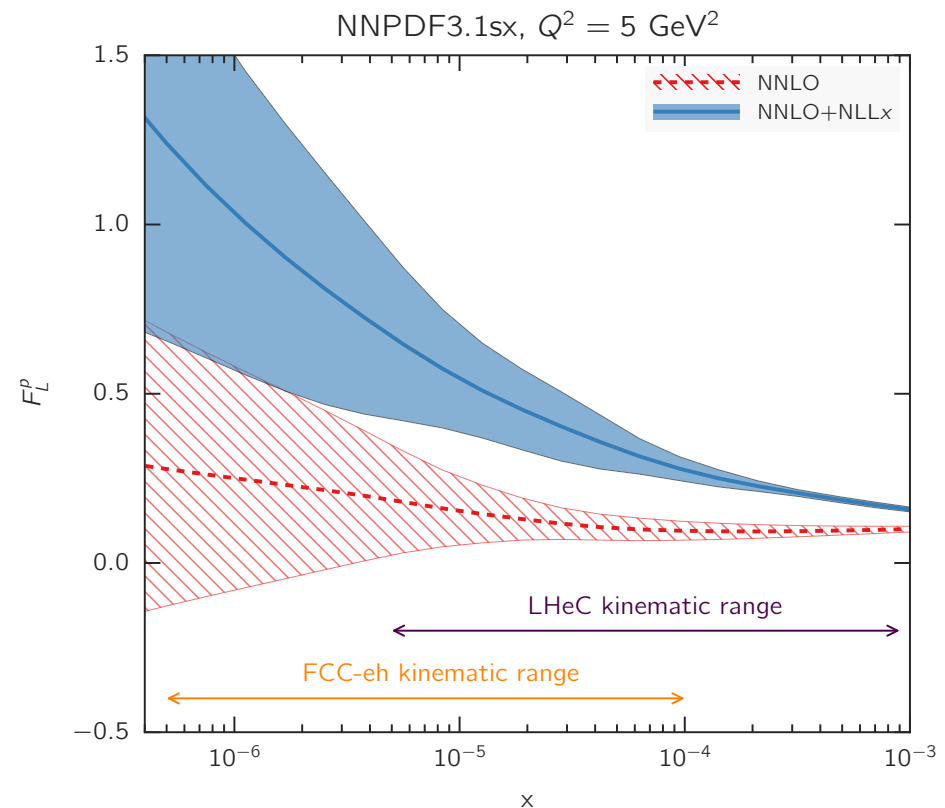
- Perform extrapolation of the calculations to the higher energy range (smaller x).
- Simulations with and without the resummation
- Compared with the pseudodata



CERN DIS proposals

LHeC: ep at $\sqrt{s} = 1.3 \text{ TeV}$, eA at $\sqrt{s} = 812 \text{ GeV}$

FCC-eh: ep at $\sqrt{s} = 3.5 \text{ TeV}$, eA at $\sqrt{s} = 2.2 \text{ TeV}$



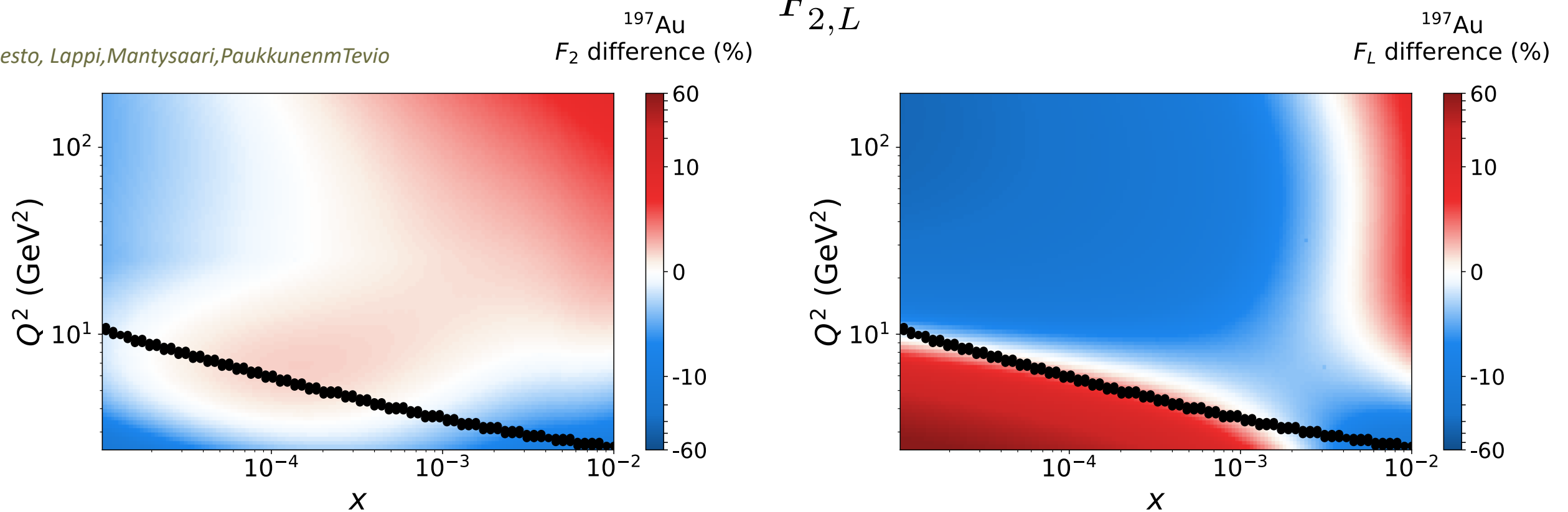
- Structure function in the LHeC/FCC-eh range can discriminate between different scenarios
- **Longitudinal structure function** particularly sensitive to the resummation vs fixed order
- **EIC**: lower energy, so likely in **preasymptotic** regime, but can measure longitudinal structure function **with precision**, thanks to **high luminosity and varying energies**

Testing saturation through inclusive structure functions at EIC

Study differences in evolution between **linear DGLAP** evolution and **nonlinear** evolution with **saturation**
Matching of both approaches in the region where saturation effects expected to be small
 Quantify differences away from the matching region: **differences in evolution dynamics**

$$\frac{F_{2,L}^{\text{BK}} - F_{2,L}^{\text{Rw}}}{F_{2,L}^{\text{BK}}}$$

Armesto, Lappi, Mantysaari, Paukkunen, Tevio



Heavy nucleus: difference between DGLAP and nonlinear are few % for F_2^A and up to 20% for F_L^A .

Longitudinal structure function can provide good sensitivity at EIC

Deep Inelastic Scattering: structure functions

Inclusive DIS cross section for $lp \rightarrow lX$ (l charged lepton, $Q^2 \ll M_Z^2$, $s \gg M_p^2$)

$$\frac{d^2\sigma}{dx dQ^2} = \frac{2\pi\alpha_{\text{em}}^2}{Q^4 x} [(1 + (1 - y)^2)F_2(x, Q^2) - y^2 F_L(x, Q^2)]$$

structure functions

$$y = \frac{p \cdot q}{p \cdot k} = Q^2 / (sx) \quad \text{inelasticity}$$

Structure functions encode all the information about the **proton(hadron) structure**

$$F_T(x, Q^2) = F_2(x, Q^2) - F_L(x, Q^2) \quad \text{transversely polarized photons}$$

$$F_L(x, Q^2) \quad \text{longitudinally polarized photons}$$

reduced cross section

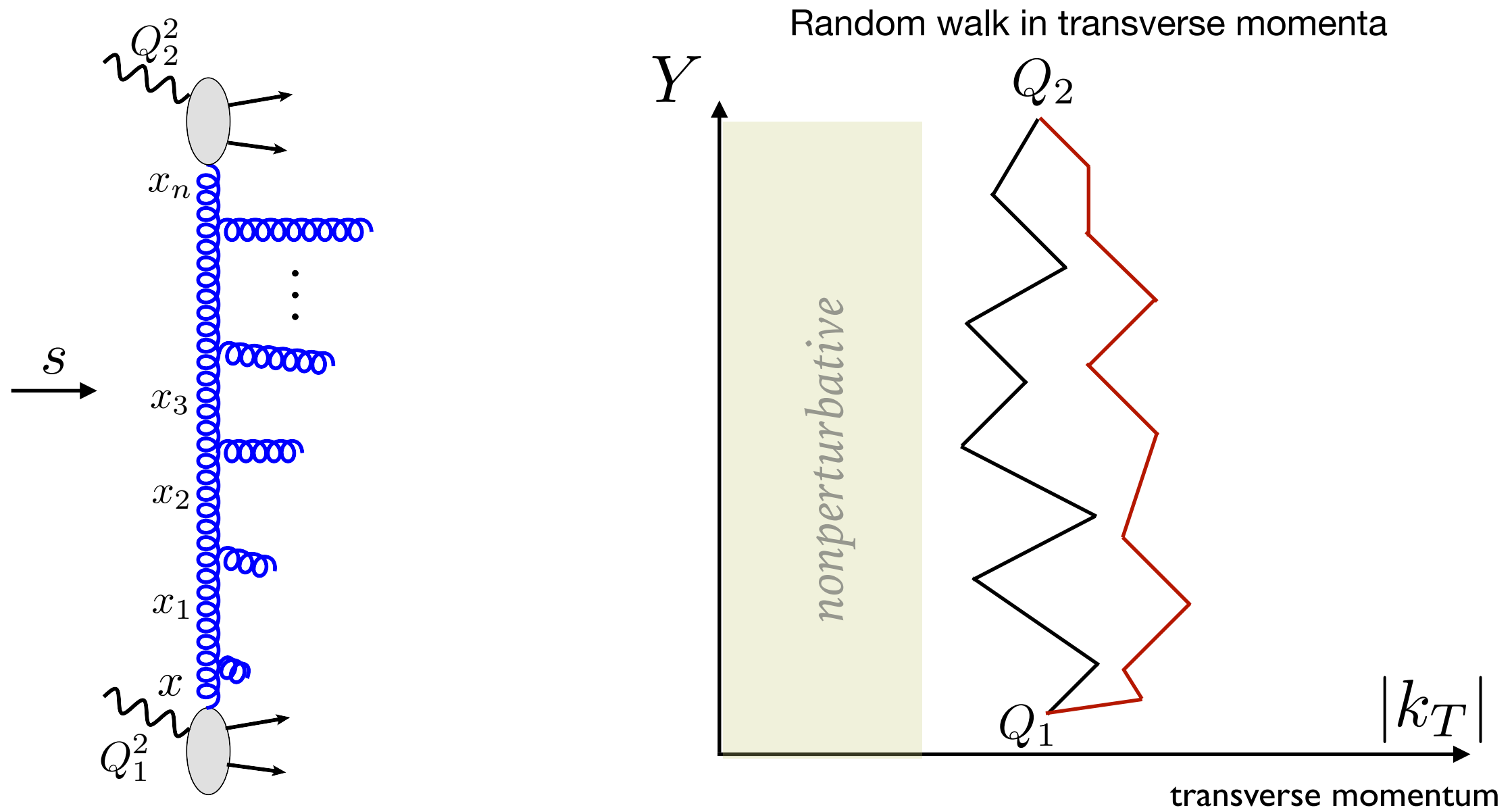
$$\sigma_{r,NC} = \frac{d^2\sigma_{NC}}{dx dQ^2} \frac{Q^4 x}{2\pi\alpha_{\text{em}} Y_+} = F_2 - \frac{y^2}{Y_+} F_L$$

$$Y_+ = 1 + (1 - y)^2$$

Measurement of F_L requires varying energies s . Possible at EIC

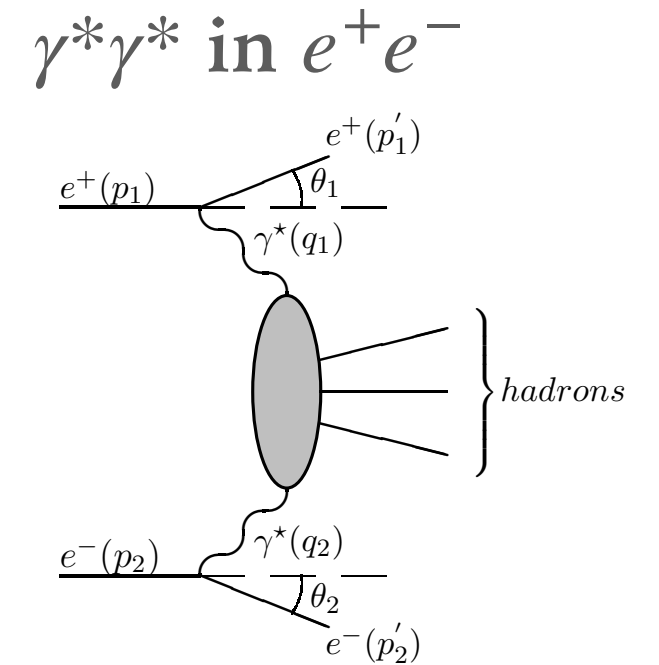
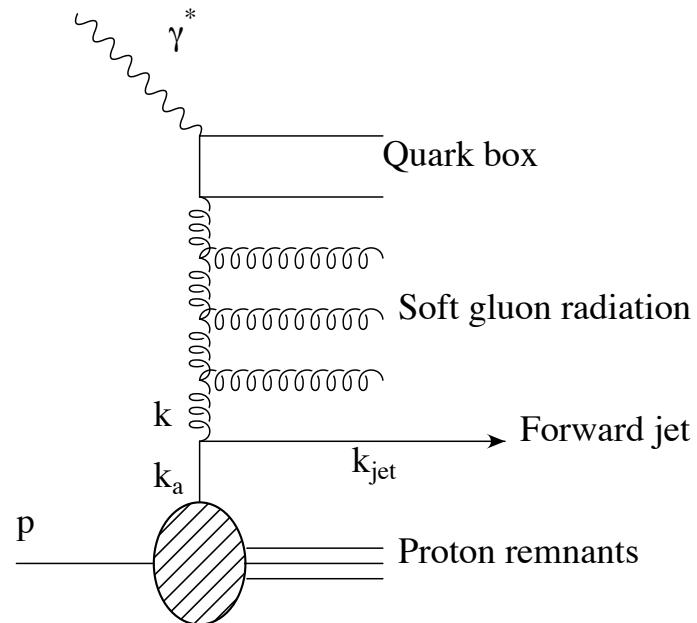
Two scale processes

Consider a process with two large scales (ex. $\gamma^*\gamma^*$ scattering, two jets,...) with $Q_1^2 \sim Q_2^2 \gg \Lambda_{QCD}^2$
 Large comparable scales to suppress DGLAP, large rapidity for BFKL evolution, keep perturbative

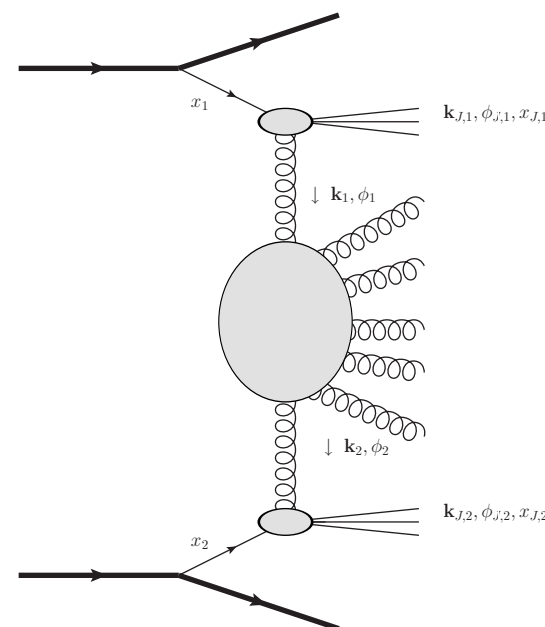


Example of two scale processes

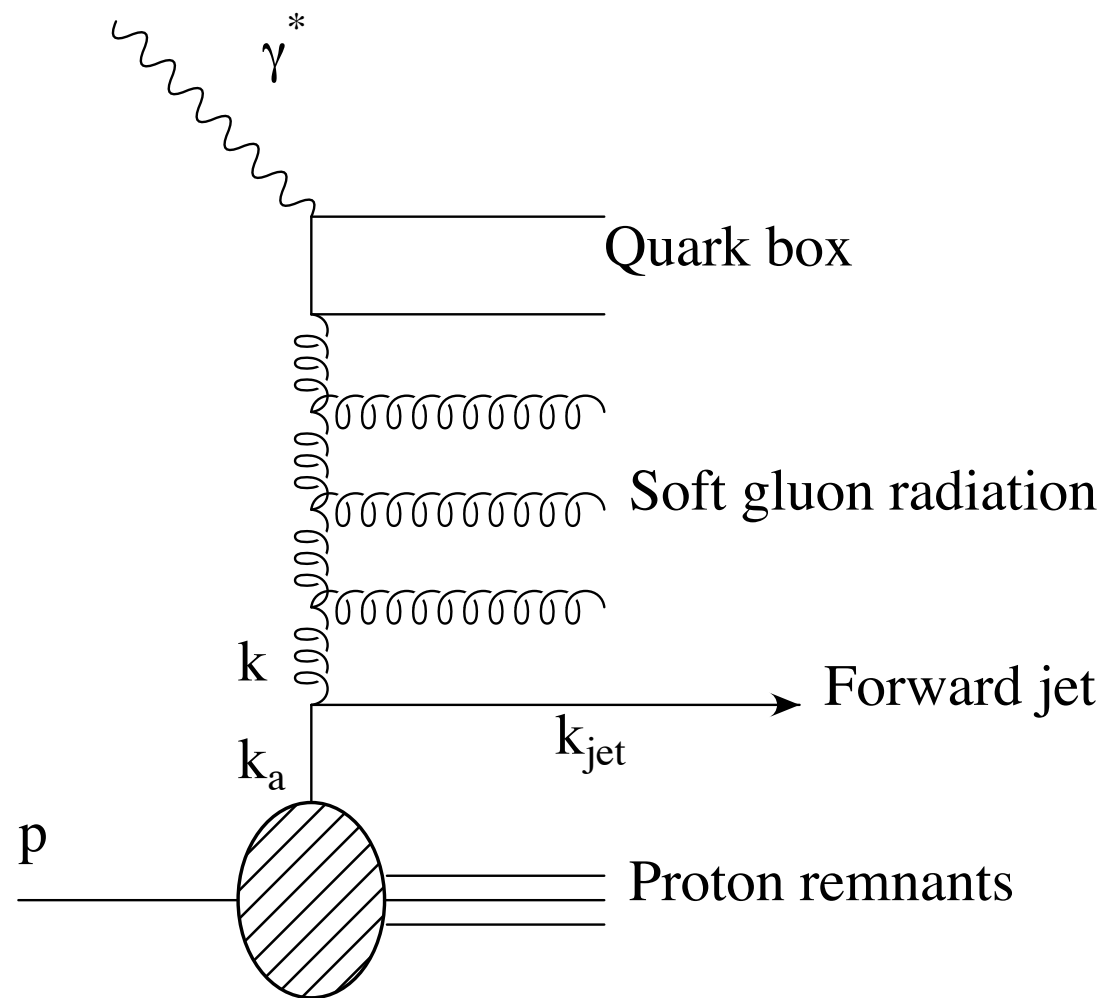
Forward jets in DIS



Mueller-Navelet in pp



Forward jet/particle in DIS



Forward jet in DIS:

$$\gamma^* + p \rightarrow \text{jet} + X$$

$$k_j = x_j^p p + x_j^\gamma q' + \mathbf{k}_{jT}$$

p four-momentum of the proton

q four-momentum of the photon

q' light-like vector: $q' = q + xp$

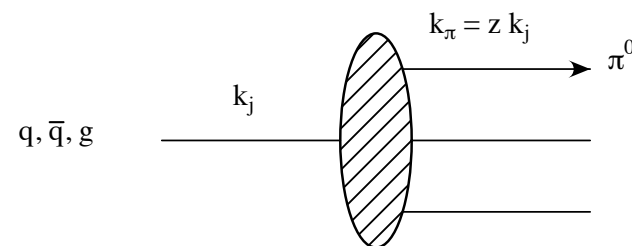
Forward jet requirement:

$$x_j \gg x \quad \text{or} \quad \ln \frac{x}{x_j} \quad \text{large}$$

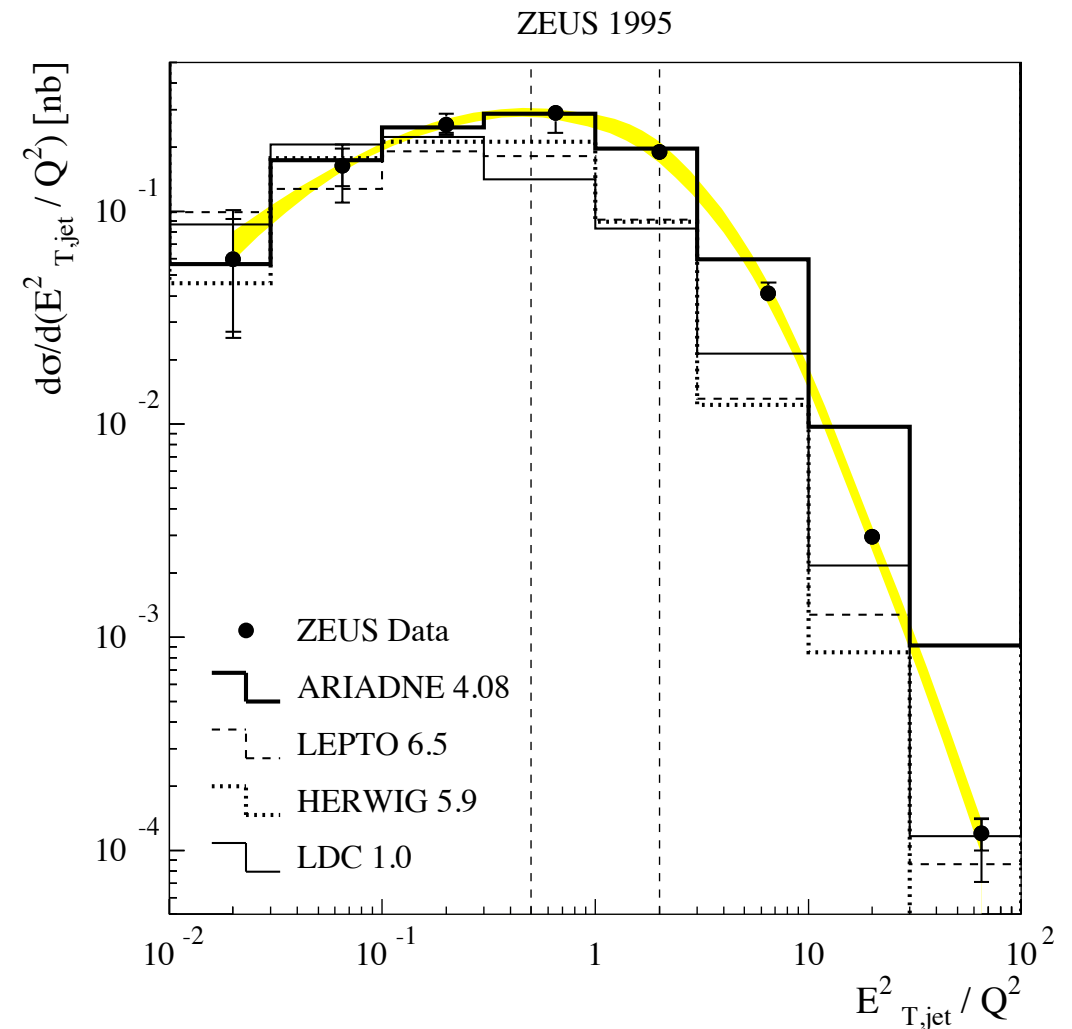
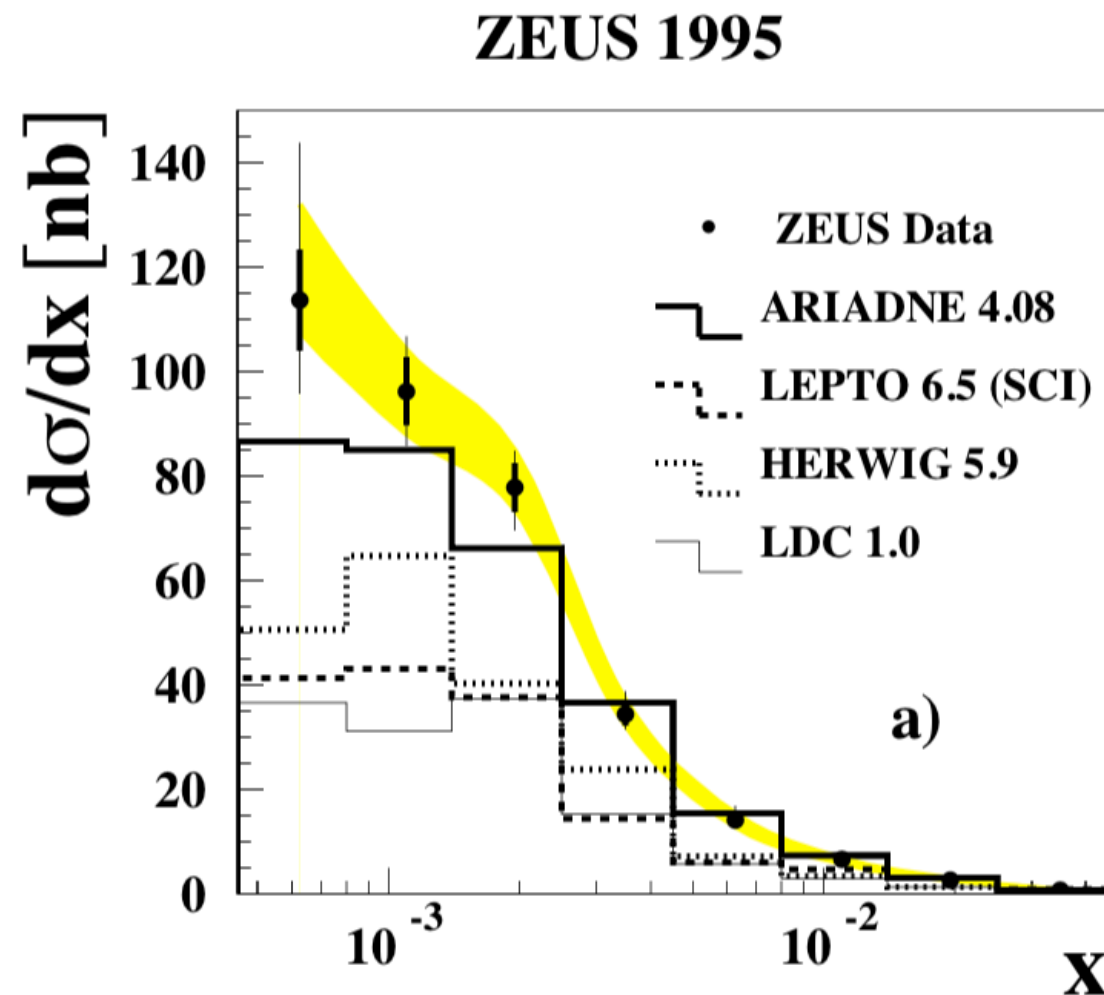
To suppress DGLAP evolution need: $Q^2 \simeq k_{jT}^2$

Another process: **forward π^0**

$$\gamma^* + p \rightarrow \pi^0 + X$$



Forward jet at HERA



Cross section increases steeply towards small x

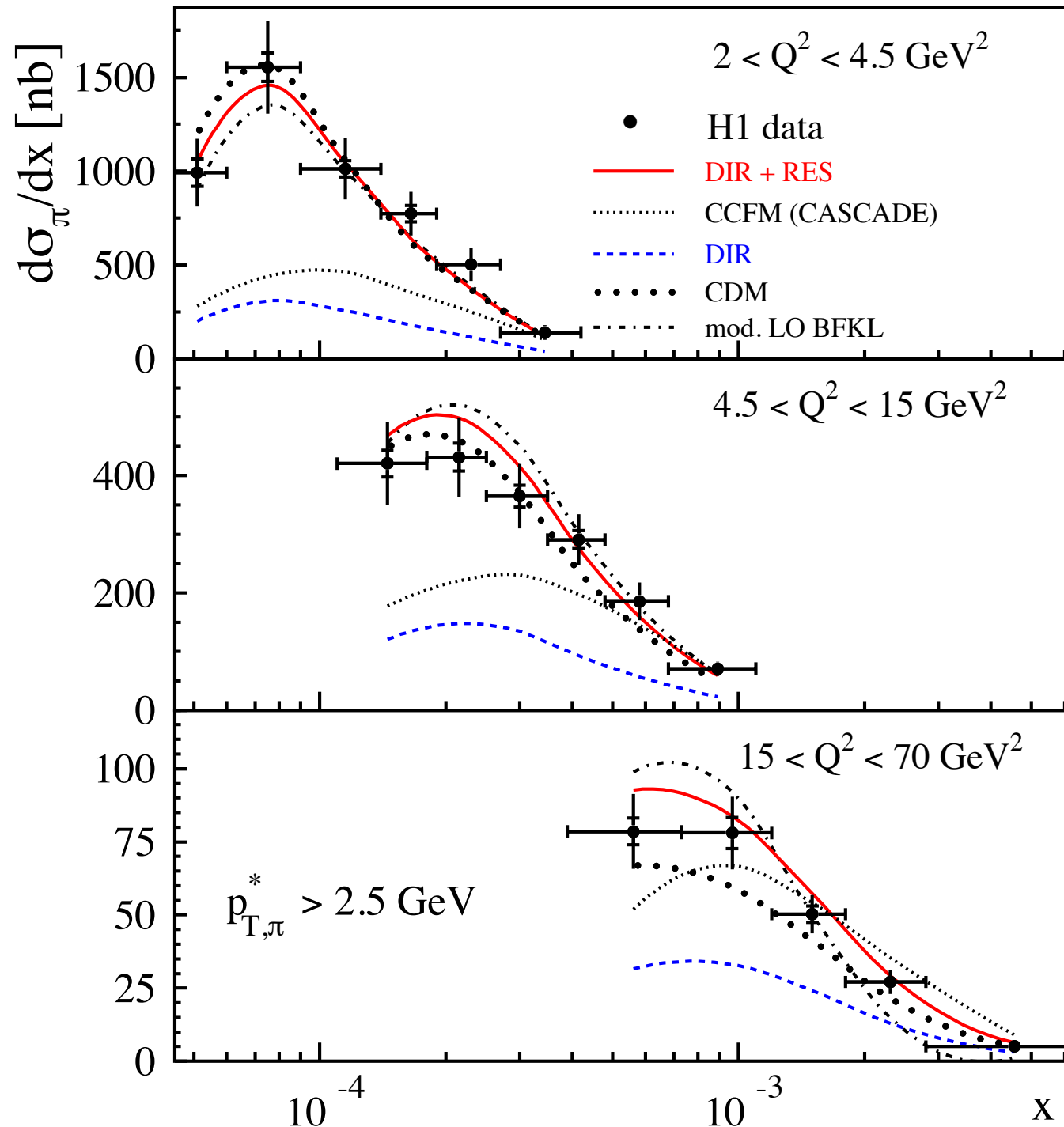
Predictions obtained from DGLAP parton shower simulations fall below measurements

ARIADNE comes close to data (has unordered emissions, similar to BFKL)

DGLAP region $E_T^2 \ll Q^2$, predictions based on DGLAP come closer to the data

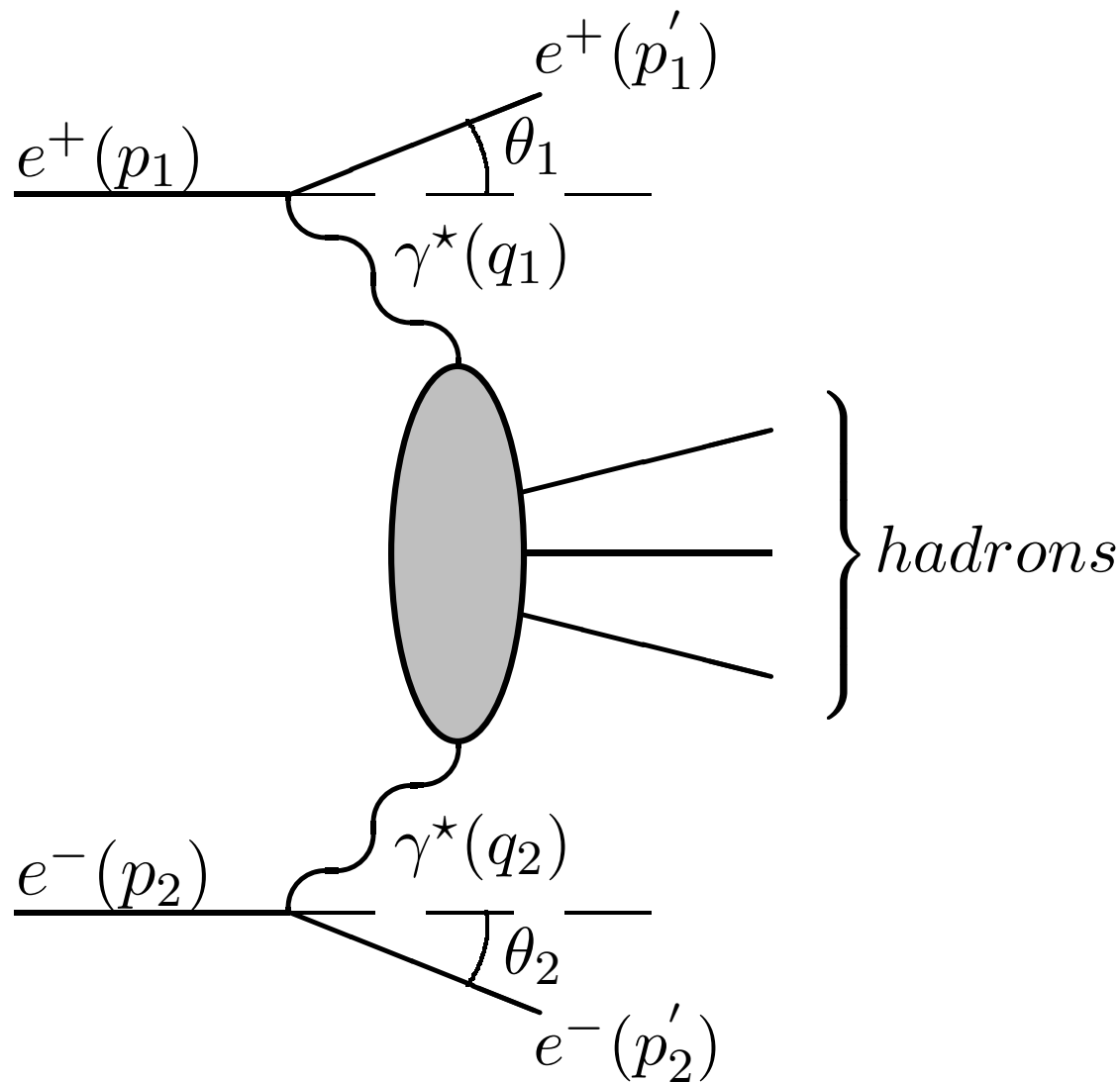
In the region, $E_T^2 \gg Q^2$, measurements tend to be above predictions

Forward π^0 in DIS



- Identified particles like π^0 allow for access to low transverse momenta and hence low x
- Calculations based on BFKL describe data well
- Also calculations which include resolved photon structure
- The latter one includes the contributions from the partonic component of the photon at low Q^2
- Can be interpreted as part of the BFKL framework

Small x at e^+e^- collider: $\gamma^*\gamma^*$ scattering into hadrons



$$Q_1^2 = -q_1^2$$

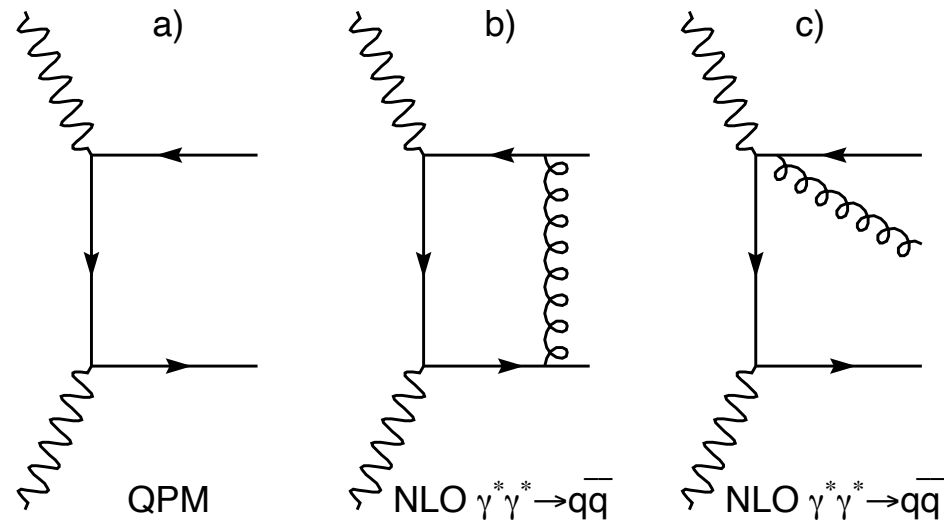
$$Q_2^2 = -q_2^2$$

$$e^+(p_1)e^-(p_2) \longrightarrow e^+(p'_1)e^-(p'_2)X$$

- Anti-tagged or no-tag (none of leptons observed): quasi-real photon scattering $Q_1^2 \sim Q_2^2 \sim 0$
- Single-tagged (one lepton observed): DIS like on a real photon $Q_1^2 \gg Q_2^2 \sim 0$
- Double-tagged (both electrons observed): high virtualities, virtual photon scattering $Q_1^2, Q_2^2 \gg 0$
- Tractable in pQCD, great process for BFKL searches if $Q_1^2 \sim Q_2^2 \gg 0$
- Measured at LEP by L3 and OPAL experiments

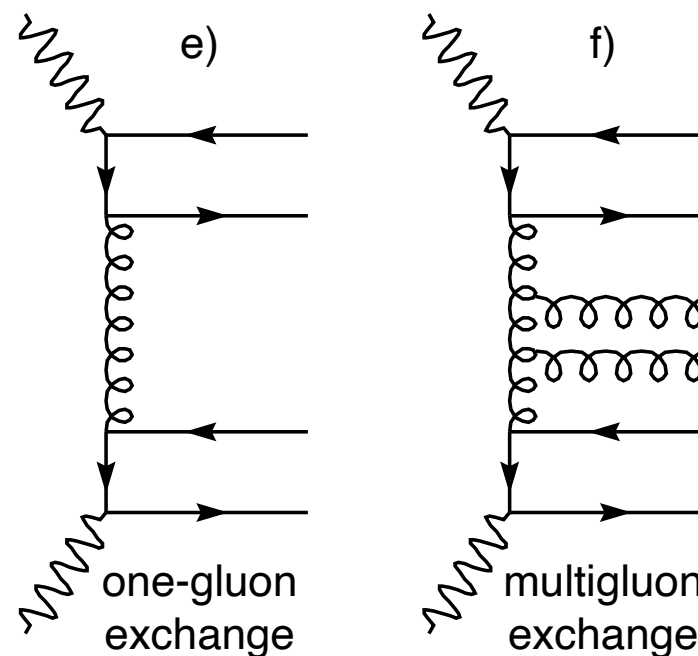
$\gamma^* \gamma^*$ scattering into hadrons: contributions

Fixed order contributions to $\gamma^* \gamma^* \rightarrow X$



Gluonic exchanges

Constant in energy: Born diagram of single gluon exchange



Exchange of BFKL Pomeron.
Process enhanced by $\alpha_s \ln s/s_0$

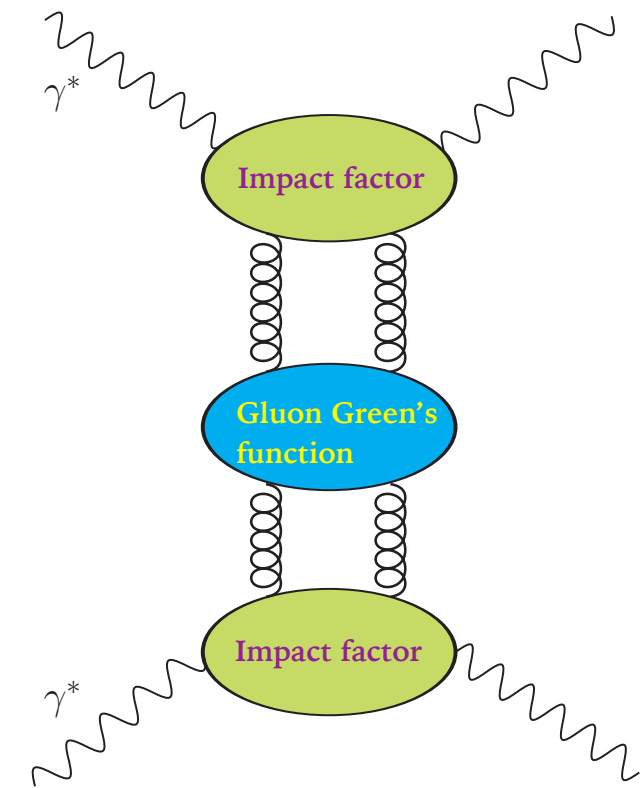
Resummation in $\gamma^*\gamma^*$ scattering

Need to apply resummation to properly describe this process

LO overestimates the data, NLO underestimates the data

Perform resummation of the gluon Green's function (evolution equation)

Perform resummation of the impact factors (currently available to NLO)



gluon Green's function
(from resummed BFKL)

$$\sigma^{(jk)}(s, Q_1, Q_2) = \frac{1}{2\pi Q_1 Q_2} \int \frac{d\omega}{2\pi i} \left(\frac{s}{s_0}\right)^\omega \int \frac{d\gamma}{2\pi i} \left(\frac{Q_1^2}{Q_2^2}\right)^{\gamma - \frac{1}{2}} \Phi^{(j)}(\omega, \gamma) \mathcal{G}(\omega, \gamma) \Phi^{(k)}(\omega, 1 - \gamma)$$

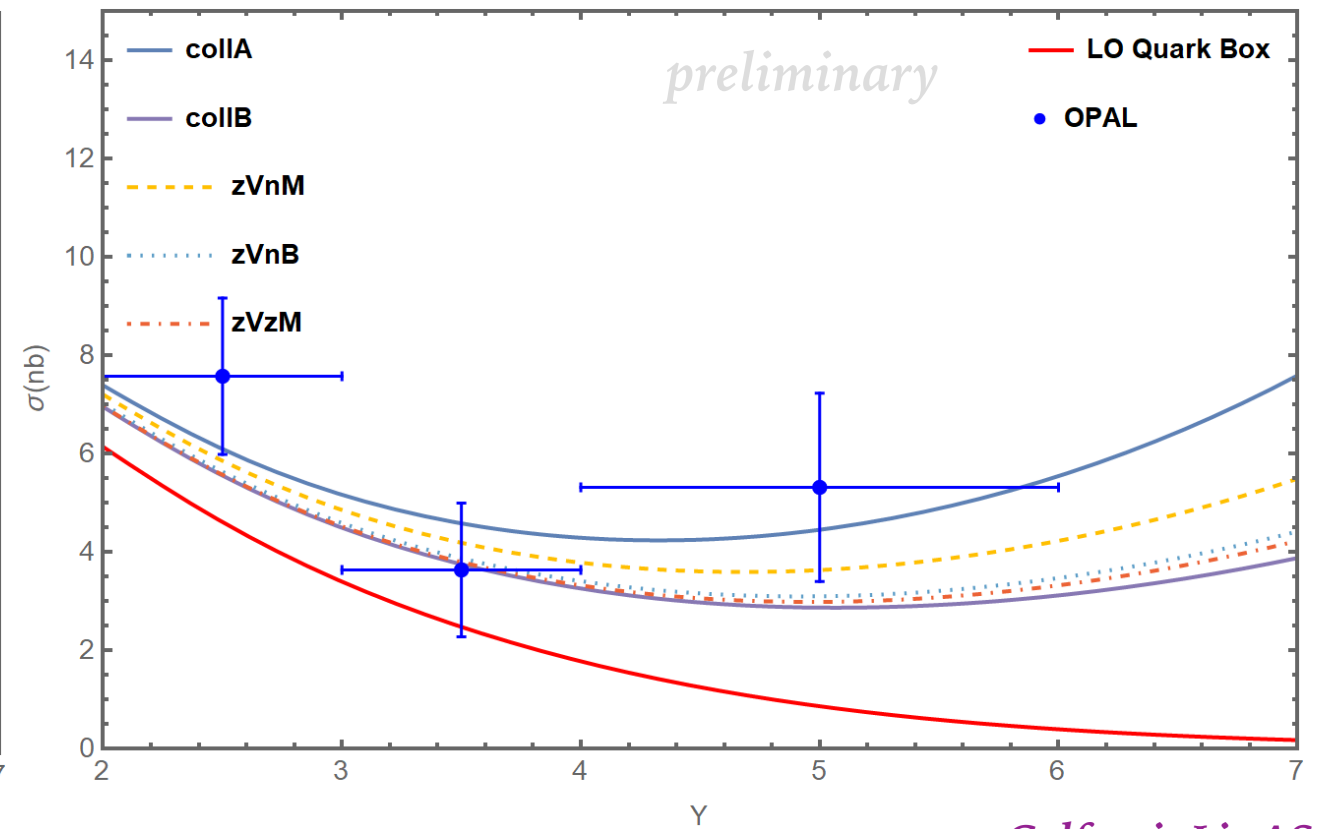
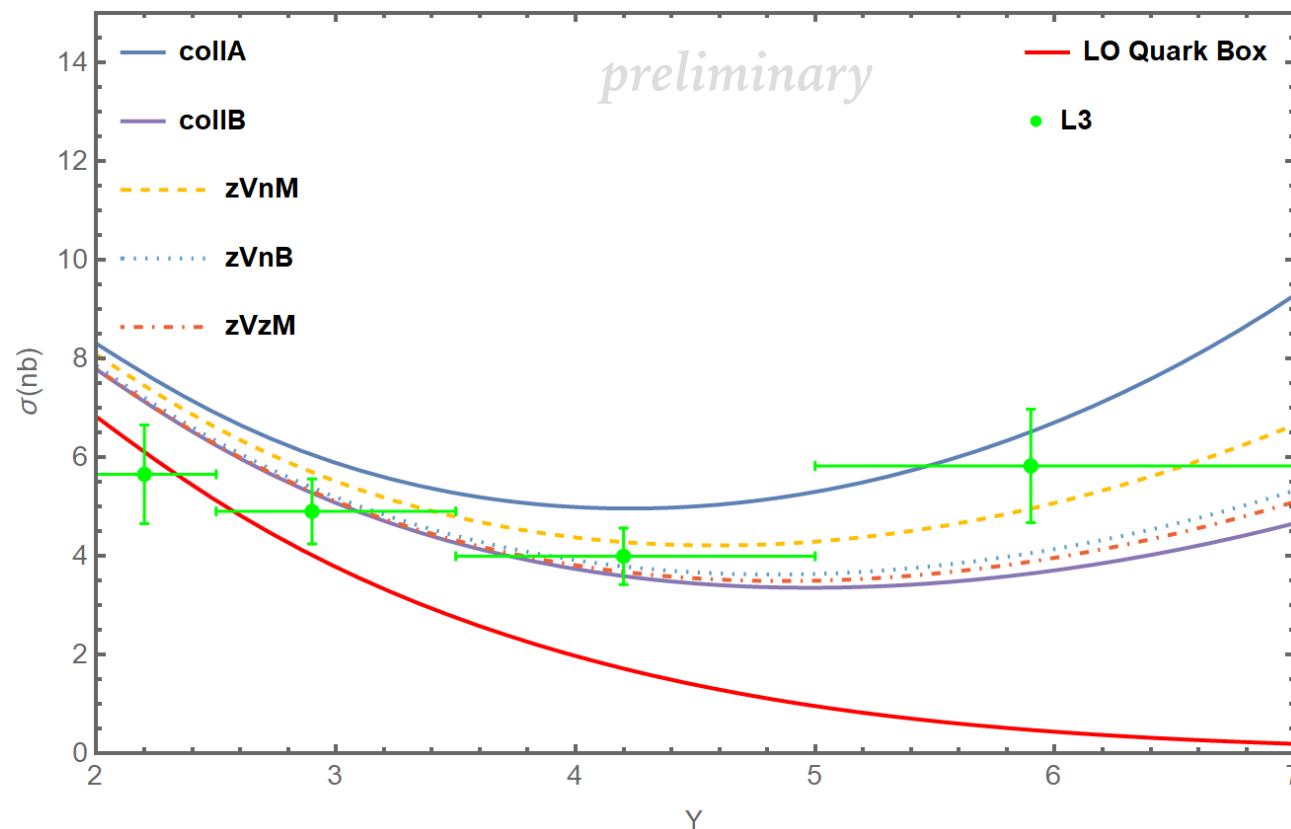
cross section

Resummed impact factors

Results for $\gamma^*\gamma^*$ cross section

L3: $Q^2 = 16 \text{ GeV}^2$

OPAL: $Q^2 = 17.9 \text{ GeV}^2$



Colferai, Li, AS

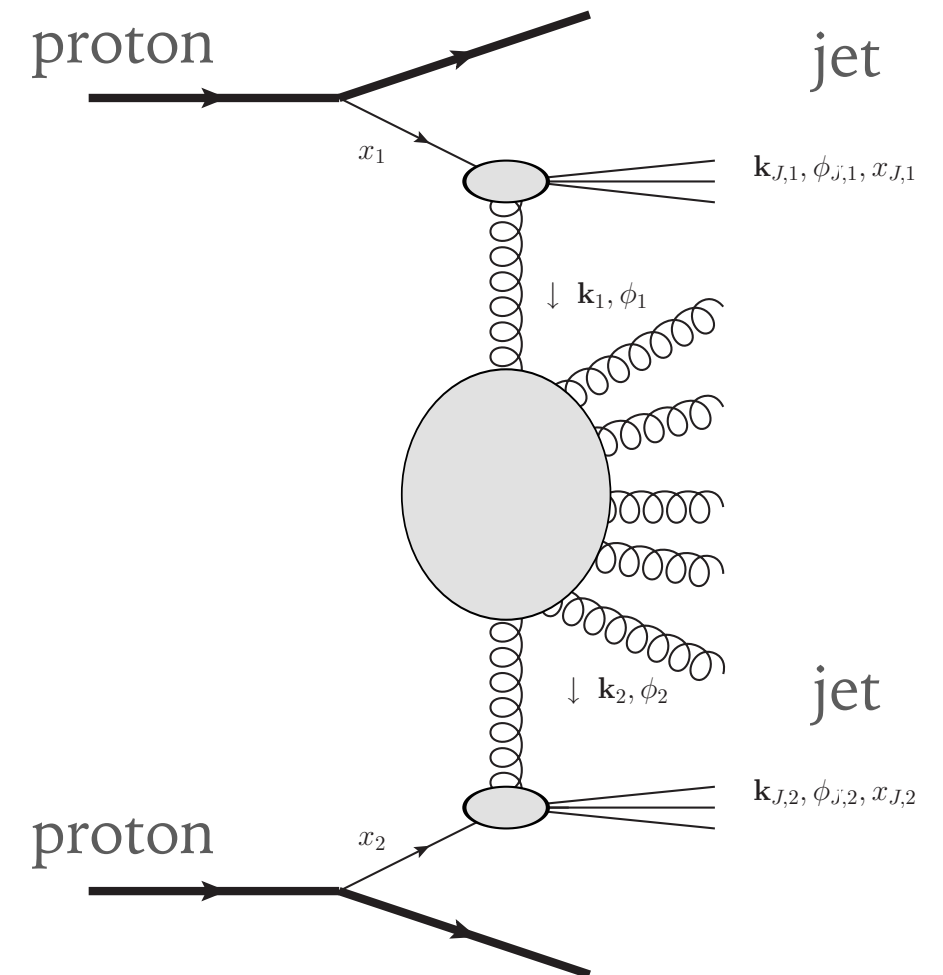
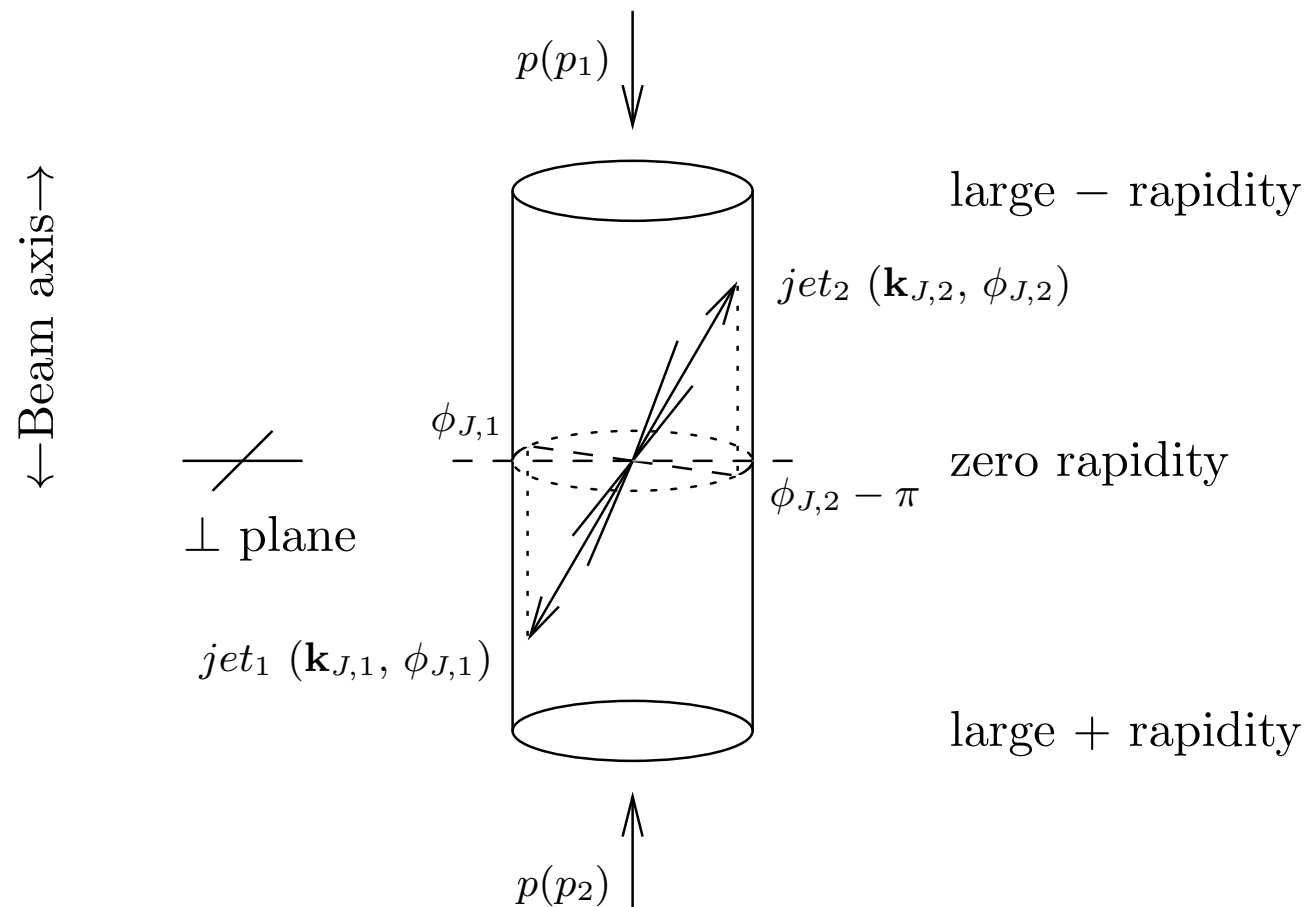
Fixed order (quark box) decreasing with energy

Overall : resummation calculation consistent with the data (LL BFKL overestimates the data, NLL underestimates)

Caveat: calculation is for $n_f = 3$ light (massless) flavors, need to include charm with mass effect

Mueller-Navelet process in proton-proton collision

Two jets in hadronic collisions separated by large rapidity: $p + p \rightarrow 2\text{jets}(\Delta Y) + X$



Large rapidity difference: phase space for BFKL evolution

Can select jets with similar transverse momenta $\mathbf{k}_{J1}^2 \sim \mathbf{k}_{J2}^2$, suppress DGLAP evolution

Can study azimuthal (de)correlations. Multiple emissions between jets will lead to decorrelation

Quantifying azimuthal (de)correlations

Decompose the cross section into Fourier series in decorrelation angle: angle between jets, minus π

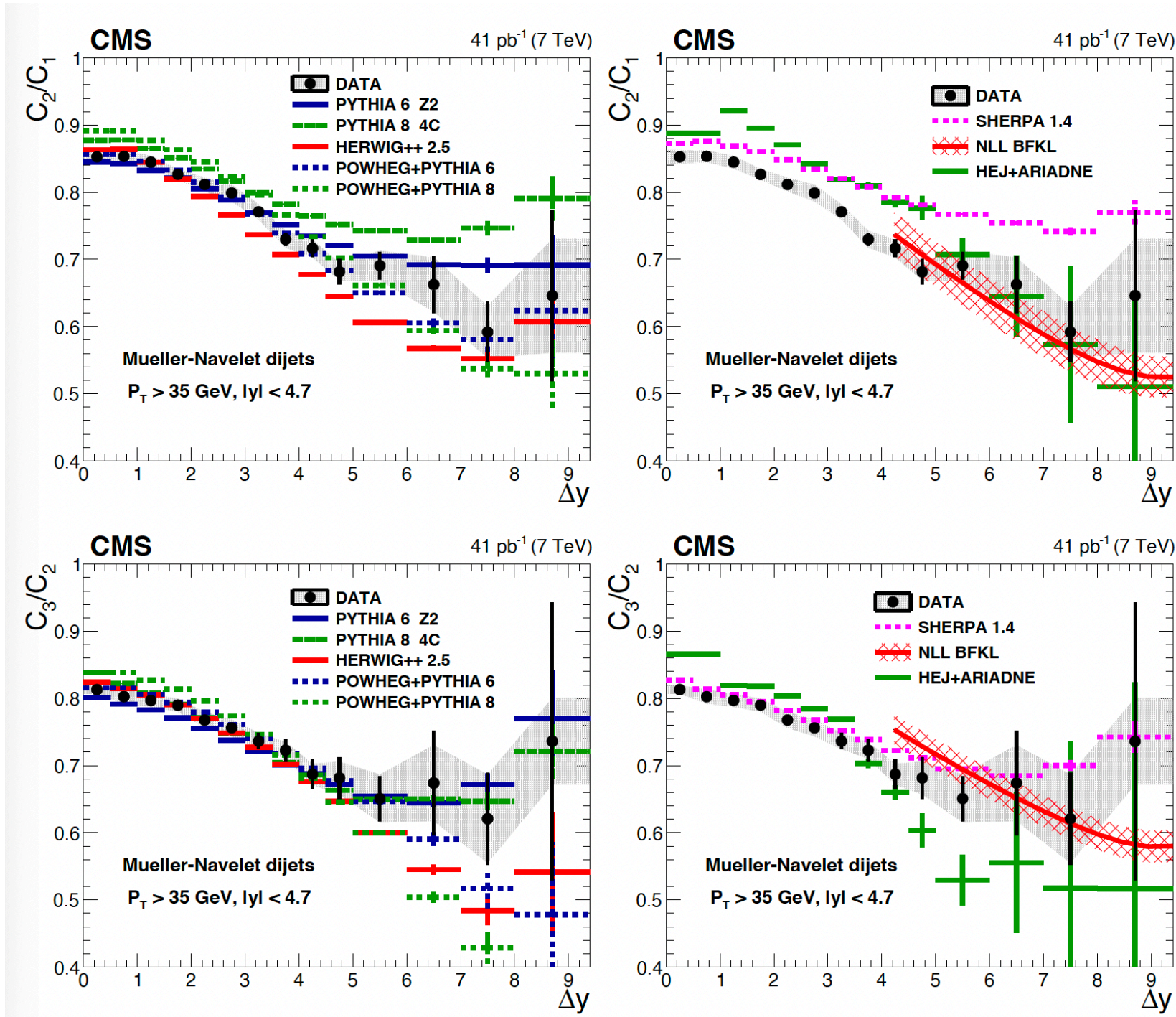
$$\frac{d\sigma}{dy_{J_1} dy_{J_2} d|\vec{k}_{J_1}| d|\vec{k}_{J_2}| d\phi_{J_1} d\phi_{J_2}} = \frac{1}{(2\pi)^2} \left[\mathcal{C}_0 + \sum_{n=1}^{\infty} 2 \cos(n\phi) \mathcal{C}_n \right]$$

where $\phi = \phi_{J_1} - \phi_{J_2} - \pi$ and the coefficient of expansion are defined by

$$\mathcal{C}_n \equiv \int_0^{2\pi} d\phi_{J_1} \int_0^{2\pi} d\phi_{J_2} \cos[n(\phi_{J_1} - \phi_{J_2} - \pi)] \frac{d\sigma}{dy_{J_1} dy_{J_2} d|\vec{k}_{J_1}| d|\vec{k}_{J_2}| d\phi_{J_1} d\phi_{J_2}}$$

- Fourier coefficients \mathcal{C}_n are equal to the average cosines of the decorrelation angle $\phi = \phi_{J_1} - \phi_{J_2} - \pi$
- **Very sensitive to parton dynamics**
- If two hard jets are in the final state, they will be **approximately back-to-back** in the azimuthal plane
- Due to **parton radiation** the angular distribution has a non-zero width determined by Fourier coefficients
- In **BFKL** one expects increasing **decorrelation** with increasing rapidity interval due to the increased parton emissions
- In DGLAP strong ordering implies that, their emission will not affect jet correlation as much and should not depend on the rapidity

Azimuthal decorrelations of Mueller-Navelet jets at LHC

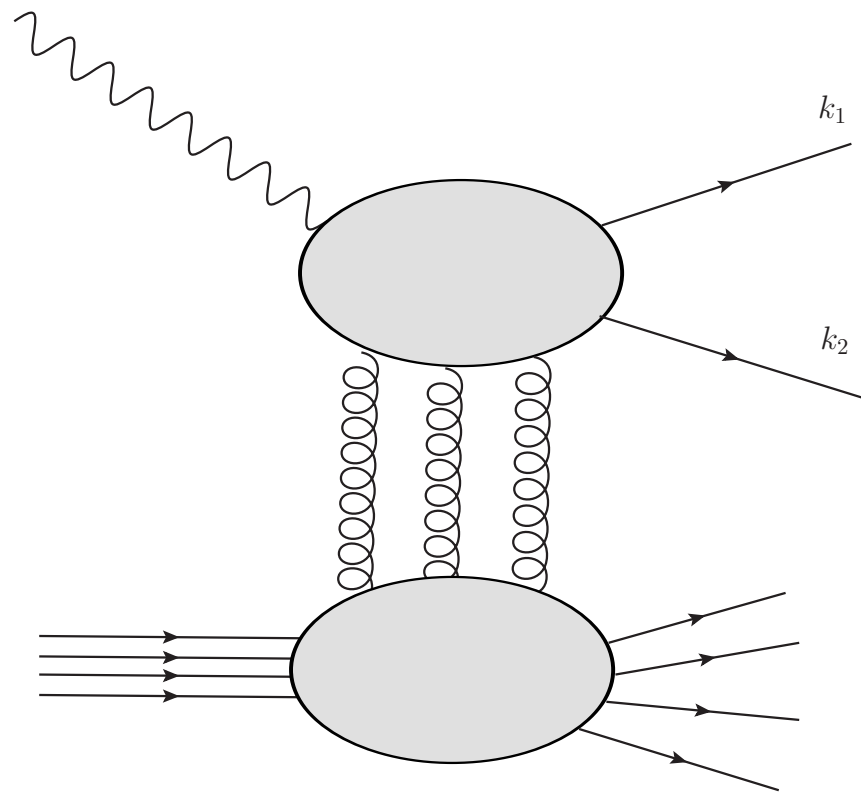


- BFKL calculation at NLL provides satisfactory description of the data at high ΔY
- MC generators provide good description at small values of ΔY , with wide spread at larger values.
- Color coherence plays important role. MPI do not seem to change the results
- More theory and experimental studies are needed

Testing small x and saturation in (de)correlations of hadrons at EIC

Azimuthal **(de)correlations of two hadrons** (dijets) in DIS in eA: direct test of the **unintegrated gluon distribution**

Instead of looking for two jets separated by large rapidity, look for two hadrons/dijets at small x



Two partons. Can look at the decorrelation of jets or hadrons

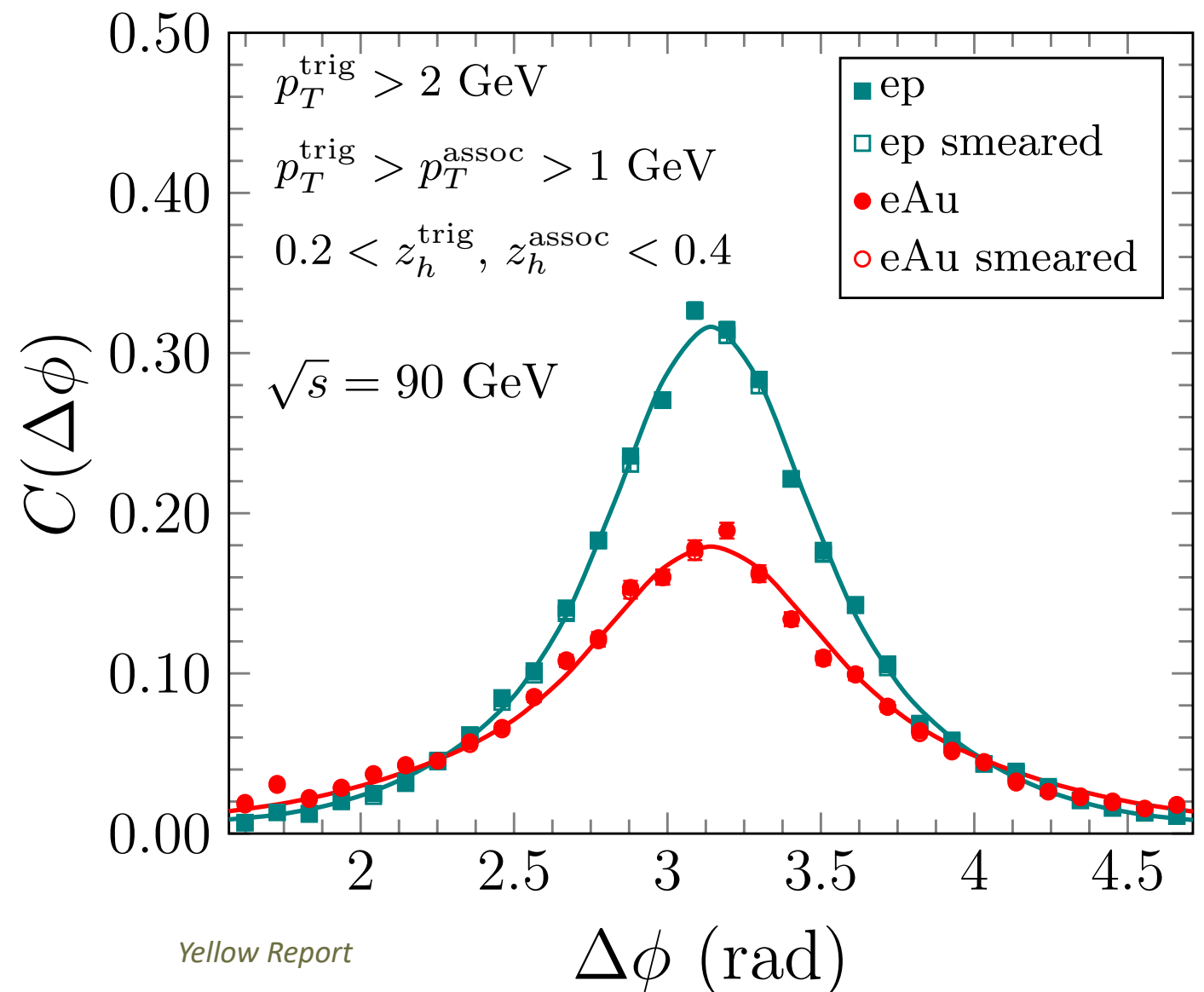
$$C(\Delta\phi) = \frac{1}{\frac{d\sigma_{\text{SIDIS}}^{\gamma^*+A \rightarrow h_1+X}}{dz_{h_1}}} \frac{d\sigma_{\text{tot}}^{\gamma^*+A \rightarrow h_1+h_2+X}}{dz_{h_1} dz_{h_2} d\Delta\phi}$$

$$\frac{d\sigma^{\gamma^*+A \rightarrow h_1+h_2+X}}{dz_{h_1} dz_{h_2} d^2p_{h_1T} d^2p_{h_2T}} \sim \mathcal{F}(x_g, q_T) \otimes \mathcal{H}(z_q, k_{1T}, k_{2T}) \otimes D_q(z_{h_1}/z_q, p_{1T}) \otimes D_q(z_{h_2}/z_q, p_{2T})$$

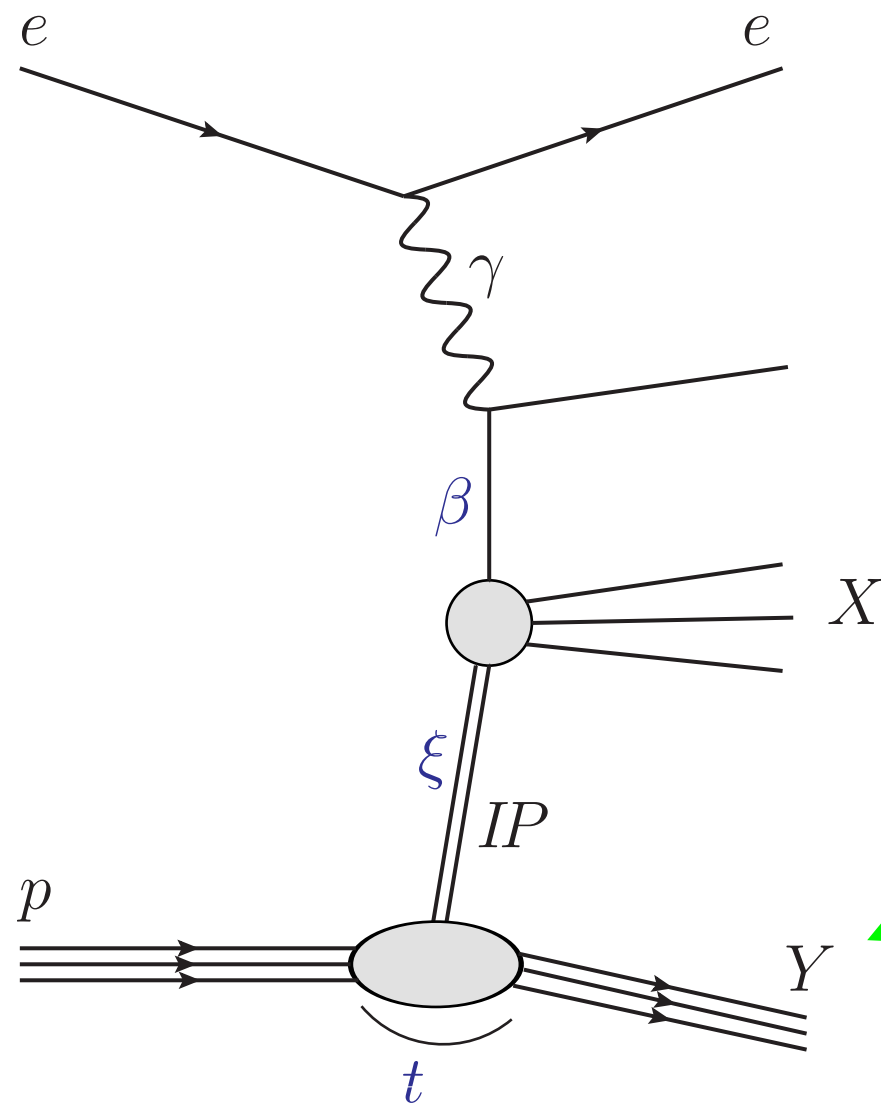
Testing small x and saturation in (de)correlations of hadrons at EIC

Clear differences between the ep and eA: **suppression** of the correlation peak in **eA** due to **saturation** effects (including the **Sudakov resummation**)

Further observables: azimuthal correlations of dihadrons/dijets in diffraction, photon+jet/dijet. These processes will allow to test various **CGC correlators**



Diffraction in DIS



Y

Final state: elastically scattered proton, or the system with the same quantum numbers

X

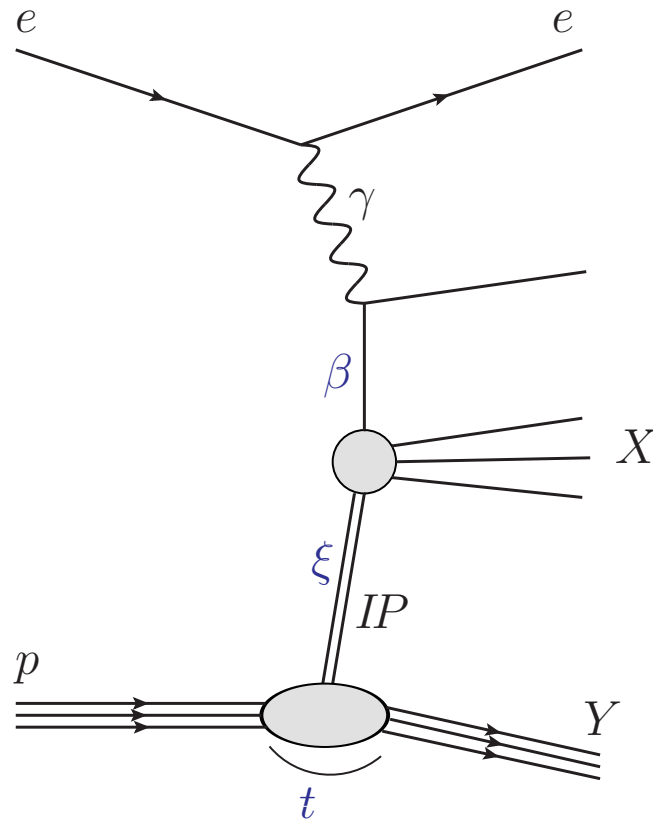
Diffractive system with mass M_x

Rapidity gap

In order for the rapidity gap to exist it needs to be mediated by the **colorless** exchange

Diffraction: a reaction characterized by a **rapidity** gap in the final state

Diffractive kinematics in DIS



Standard DIS variables:

electron-proton

cms energy squared:

$$s = (k + p)^2$$

photon-proton

cms energy squared:

$$W^2 = (q + p)^2$$

inelasticity

$$y = \frac{p \cdot q}{p \cdot k}$$

Bjorken x

$$x = \frac{-q^2}{2p \cdot q}$$

(minus) photon virtuality

$$Q^2 = -q^2$$

Target is scattered elastically:
elastic scattering

It can also dissociate into a
state Y with the same quantum
numbers, but still separated
from the rest of particles

Diffractive DIS variables:

$$\xi \equiv x_{IP} = \frac{Q^2 + M_X^2 - t}{Q^2 + W^2}$$

$$\beta = \frac{Q^2}{Q^2 + M_X^2 - t}$$

$$t = (p - p')^2$$

momentum fraction of the
Pomeron w.r.t hadron

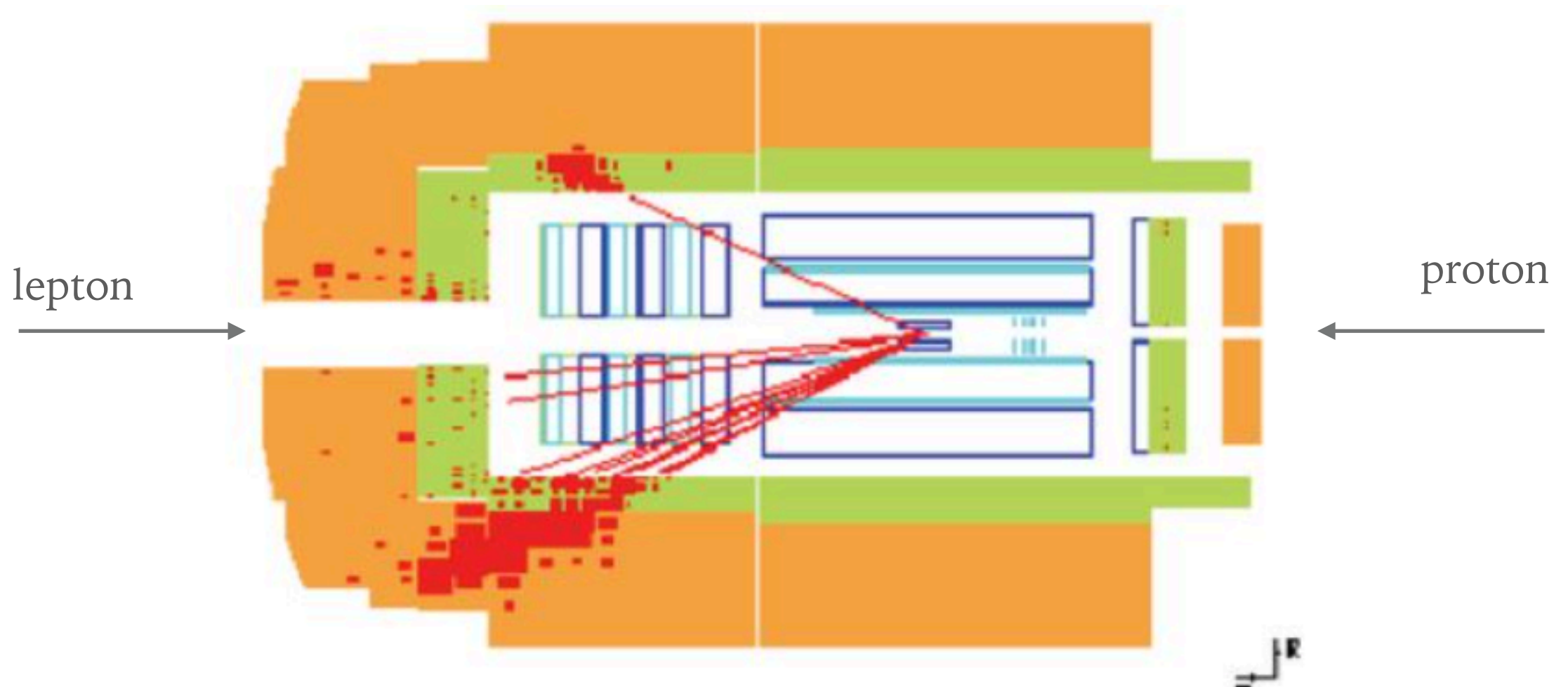
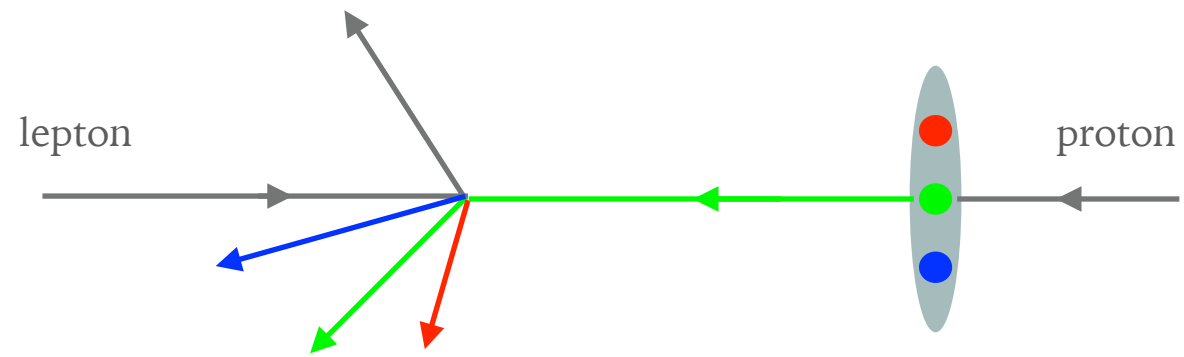
momentum fraction of parton
w.r.t Pomeron

4-momentum transfer squared

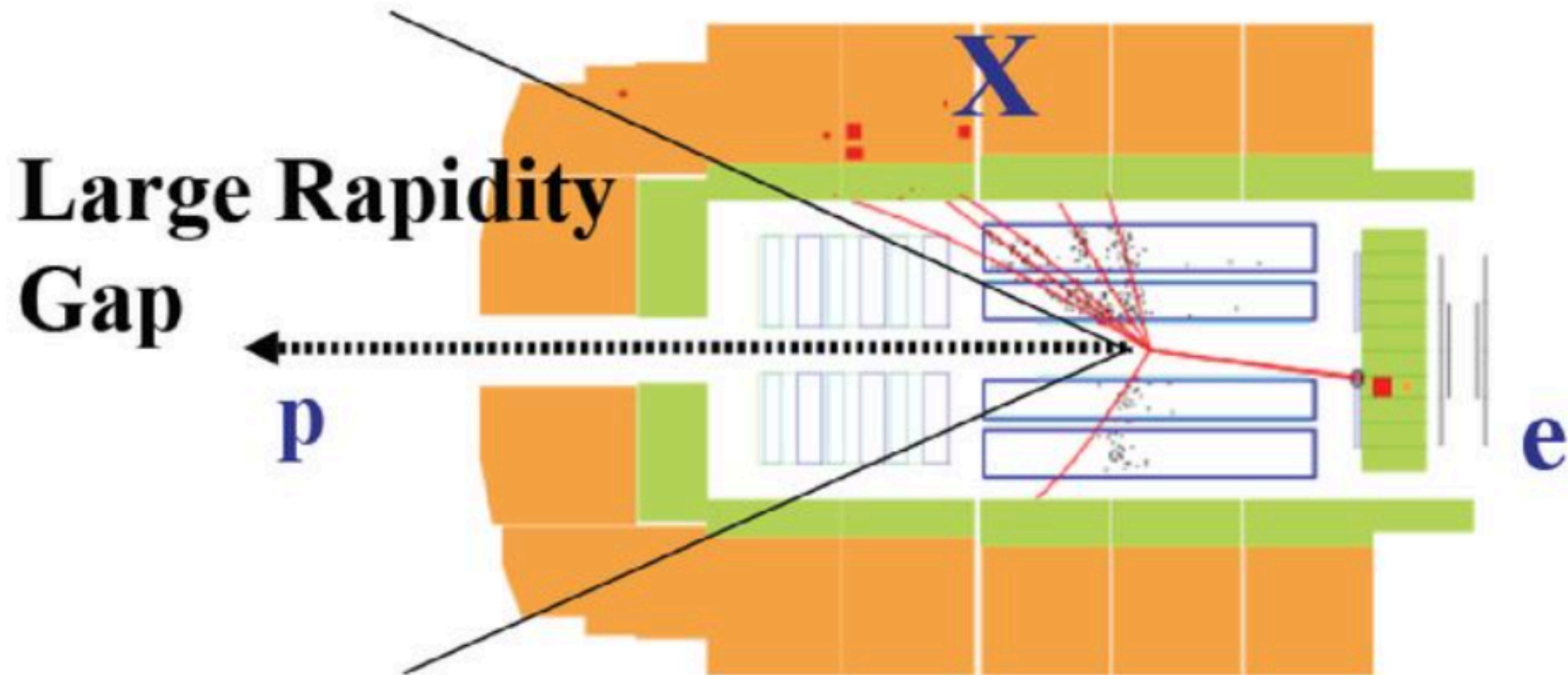
$$x = \xi \beta$$

Deep Inelastic Scattering : non-diffractive

Non-diffractive DIS event



Diffraction at HERA



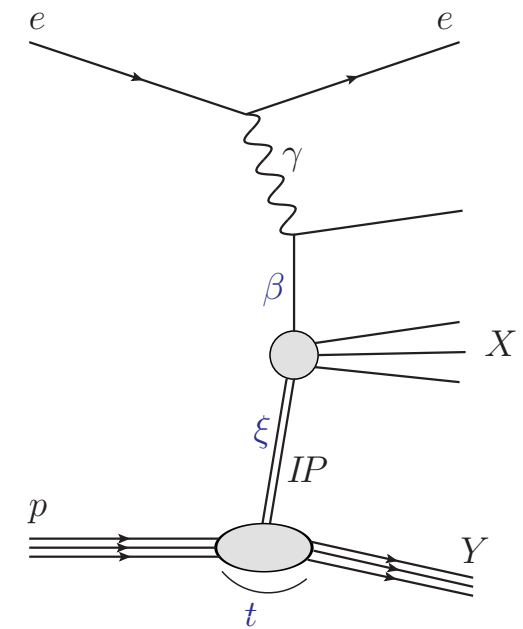
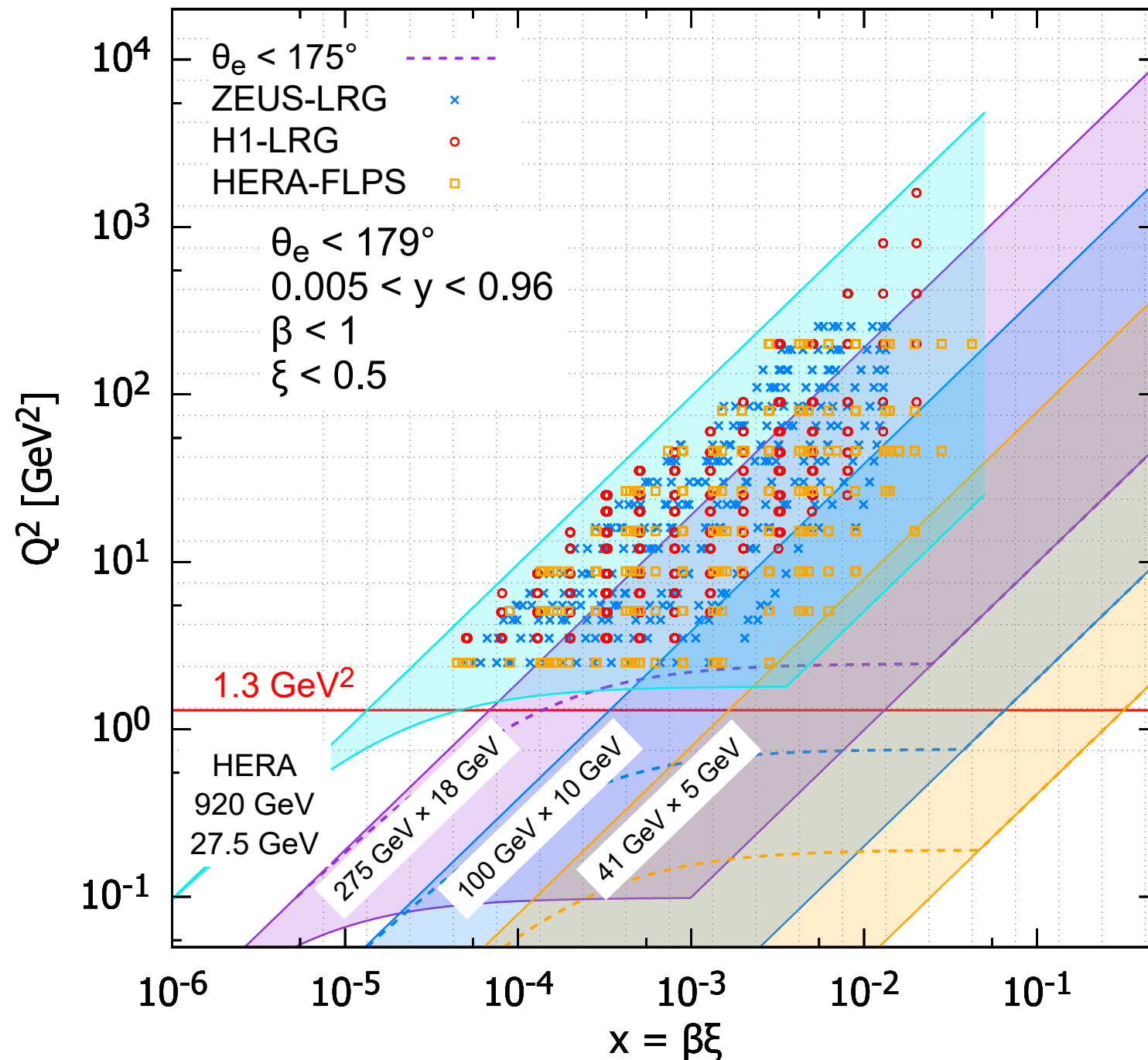
10% events at HERA were of diffractive type

Large portion of the detector void of any particle activity: **rapidity gap**

Proton stays intact despite undergoing violent collision with a 50 TeV electron (in its rest frame)

Phase space (x, Q^2) EIC-HERA in diffraction

EIC 3 scenarios - HERA



$$\xi \equiv x_{IP} = \frac{Q^2 + M_X^2 - t}{Q^2 + W^2}$$

$$\beta = \frac{Q^2}{Q^2 + M_X^2 - t}$$

$$t = (p - p')^2$$

Diffractive cross section, structure functions

Diffractive cross section depends on 4 variables (ξ, β, Q^2, t) :

$$\frac{d^4 \sigma^D}{d\xi d\beta dQ^2 dt} = \frac{2\pi\alpha_{\text{em}}^2}{\beta Q^4} Y_+ \sigma_r^{\text{D}(4)}(\xi, \beta, Q^2, t)$$

$$Y_+ = 1 + (1 - y)^2$$

Reduced cross section depends on two structure functions:

$$\sigma_r^{\text{D}(4)}(\xi, \beta, Q^2, t) = F_2^{\text{D}(4)}(\xi, \beta, Q^2, t) - \frac{y^2}{Y_+} F_L^{\text{D}(4)}(\xi, \beta, Q^2, t)$$

Upon integration over t :

$$F_{2,L}^{\text{D}(3)}(\xi, \beta, Q^2) = \int_{-\infty}^0 dt F_{2,L}^{\text{D}(4)}(\xi, \beta, Q^2, t)$$

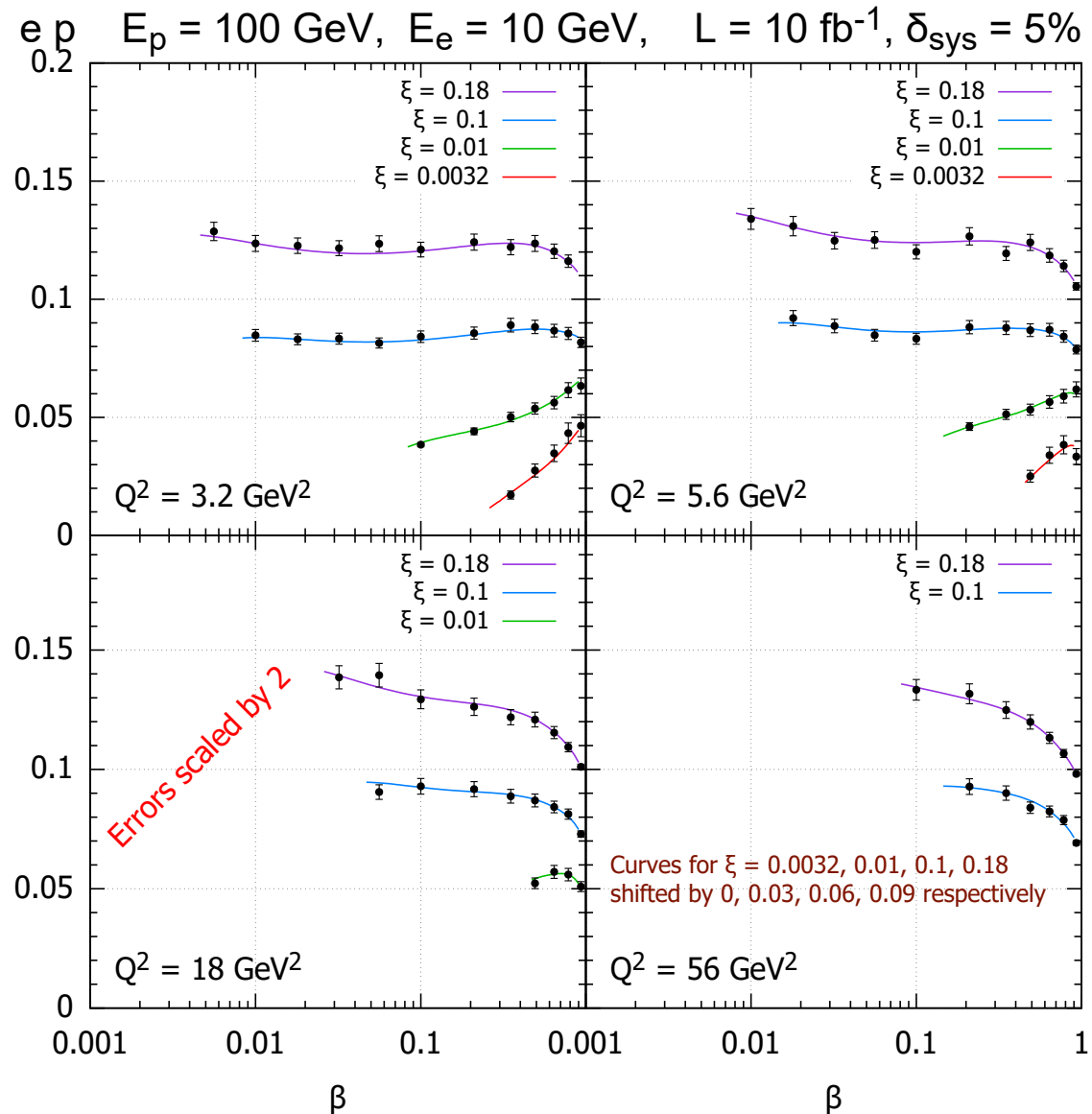
Dimensions:

$$[\sigma_r^{\text{D}(4)}] = \text{GeV}^{-2}$$

$$\sigma_r^{\text{D}(3)} \quad \text{Dimensionless}$$

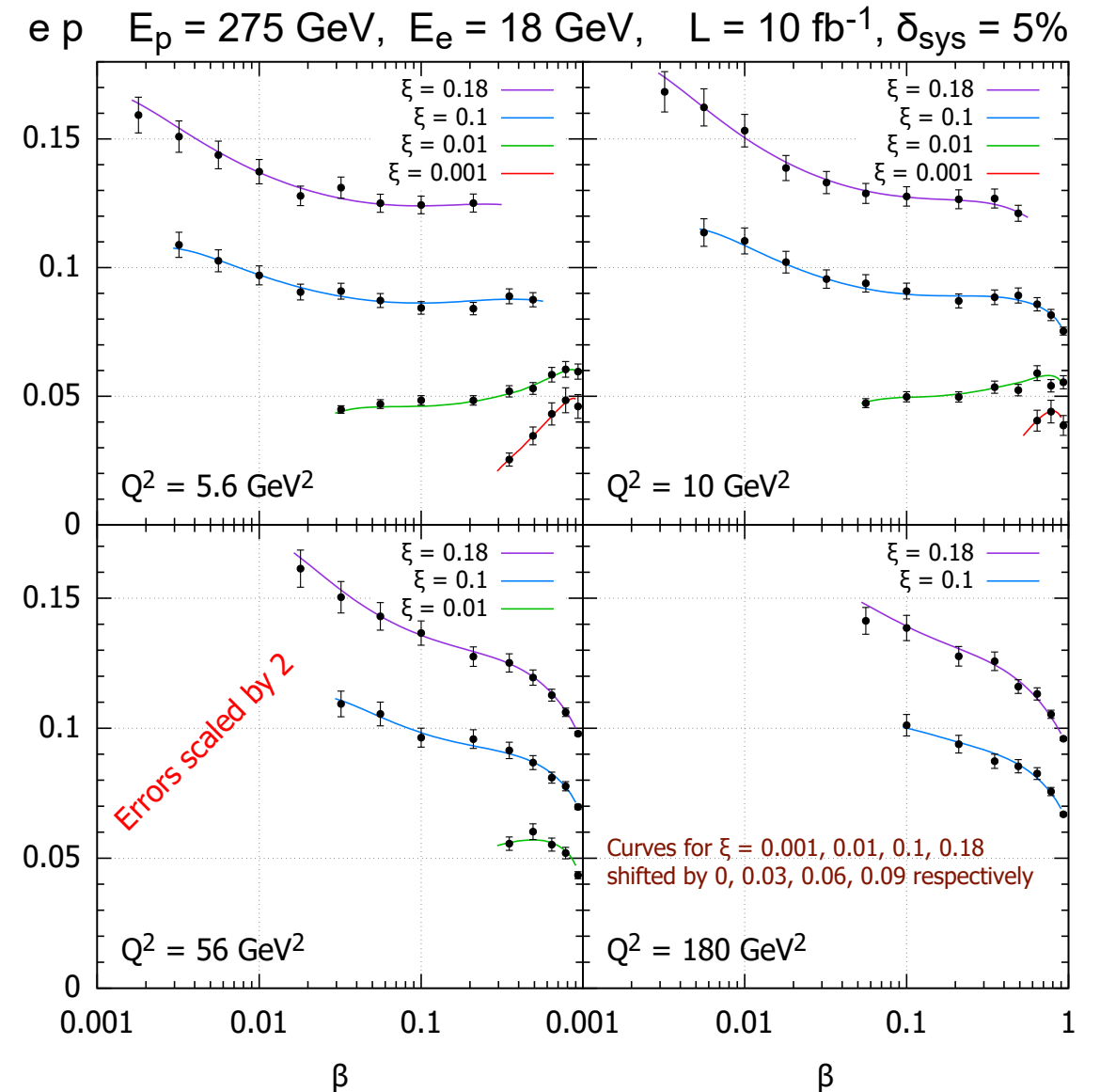
Example: pseudodata for $\sigma^{D(3)}$ in ep at EIC

Armesto, Newman, Slominski, Stasto



In total:

482 points for $1.3 < Q^2 < 1330 \text{ GeV}^2$



In total:

792 points for $1.3 < Q^2 < 4220 \text{ GeV}^2$

Possibilities for $F_L^{D(3)}$ at EIC

Why F_L^D is interesting?

$$\sigma_r^{D(3)} = F_2^{D(3)} - \frac{y^2}{Y_+} F_L^{D(3)}$$

F_L^D vanishes in the parton model

Gets non-vanishing contributions in QCD

As in inclusive case, particularly sensitive to the diffractive **gluon density**

Expected large **higher twists**, provides test of the **non-linear, saturation** phenomena

Experimentally challenging...

Measurement requires several beam energies

F_L^D strongest when $y \rightarrow 1$. Low electron energies

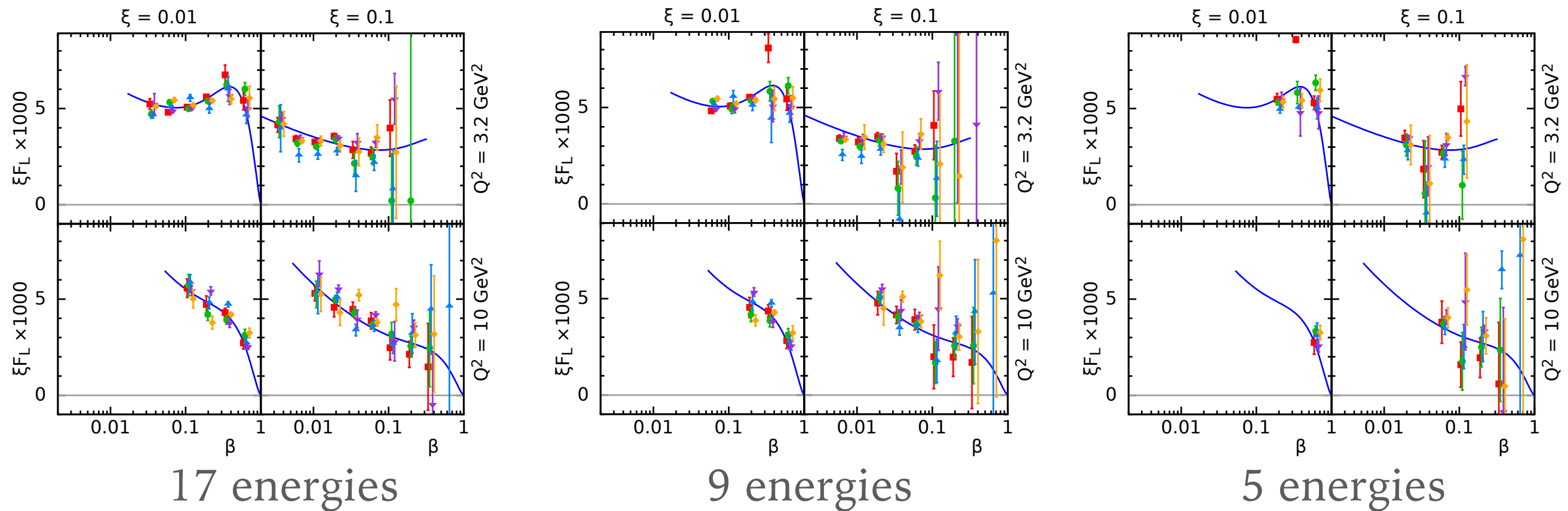
H1 measurement: 4 energies, $E_p=920, 820, 575, 460$ GeV, electron beam $E_e=27.6$ GeV

Large errors, limited by statistics at HERA

Careful evaluation of systematics. Best precision 4%, with uncorrelated sources as low as 2%

Simulated measurement of $F_L^{D(3)}$ vs β in bins of (ξ, Q^2)

Uncorr. systematic error 1%, 5 MC samples to illustrate fluctuations



Armesto, Newman, Slominski, Stasto

Small differences between S-17 and S-9, small reduction to range and increase in uncertainties.

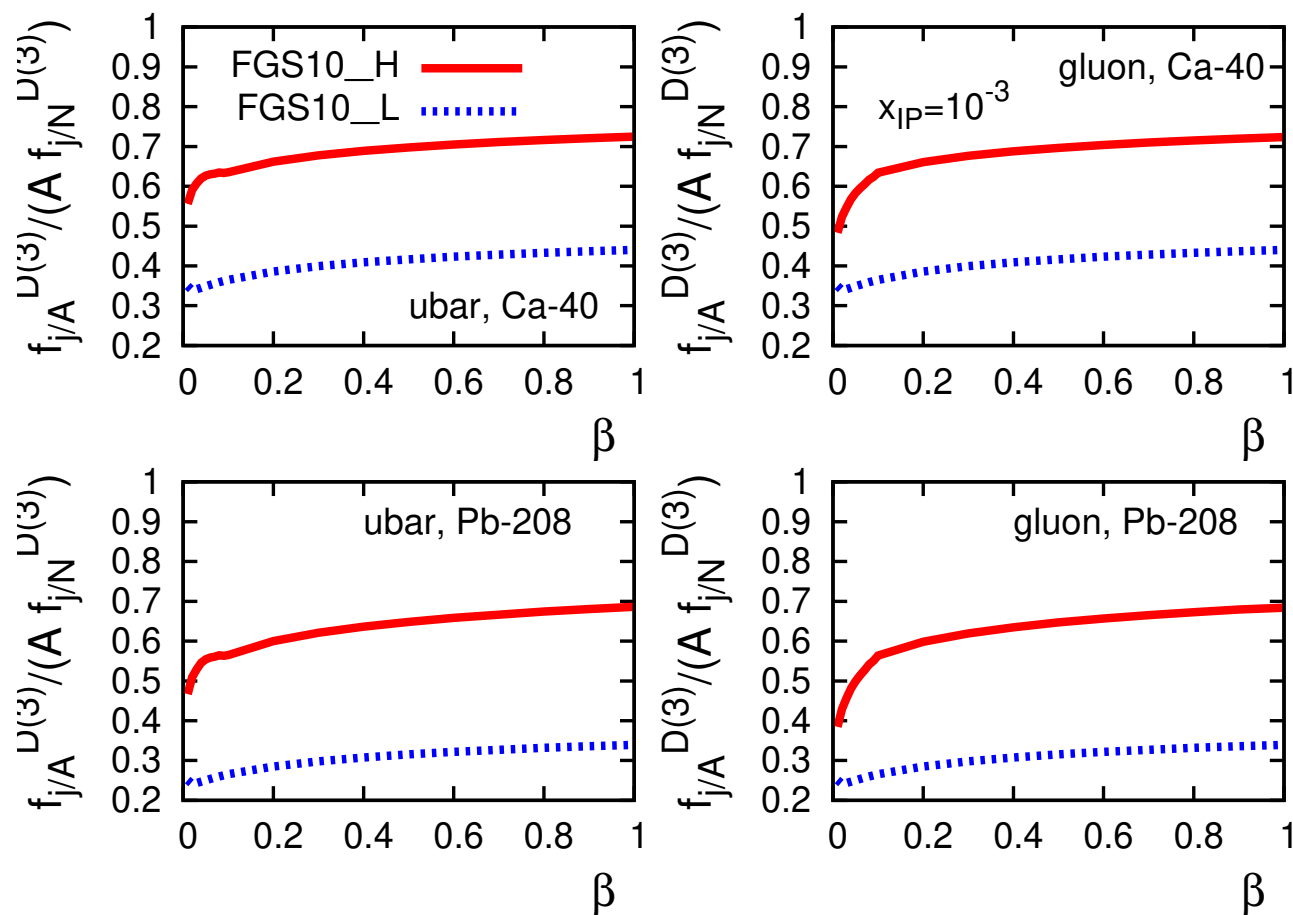
More pronounced reduction in range and higher uncertainties in S-5.

An extraction of $F_L^{D(3)}$ possible with EIC-favored set of energy combinations

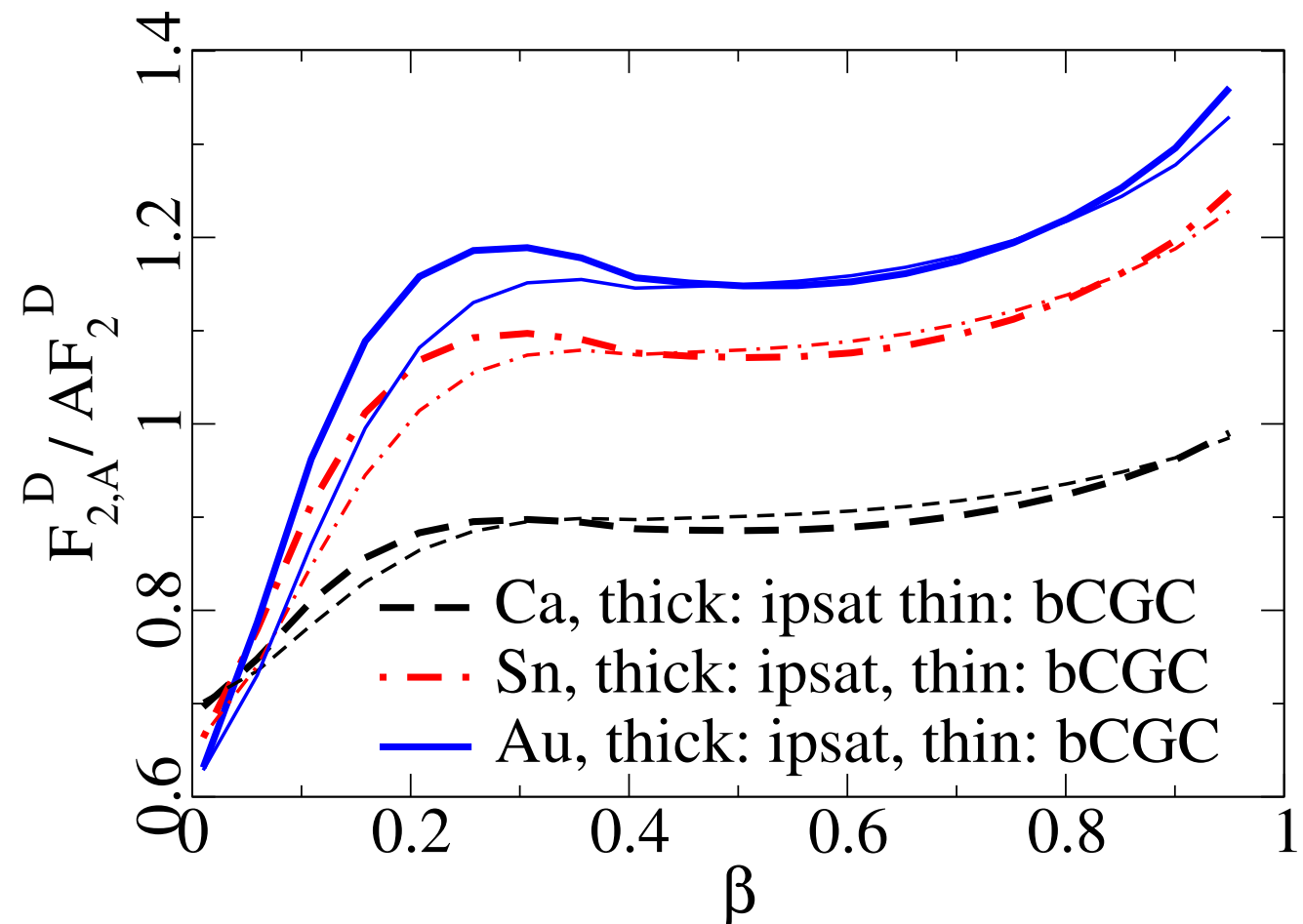
Example : inclusive diffraction in eA DIS

Diffraction to inclusive ratio of cross sections **sensitive probe to different models**

Ratio in LT shadowing : suppression



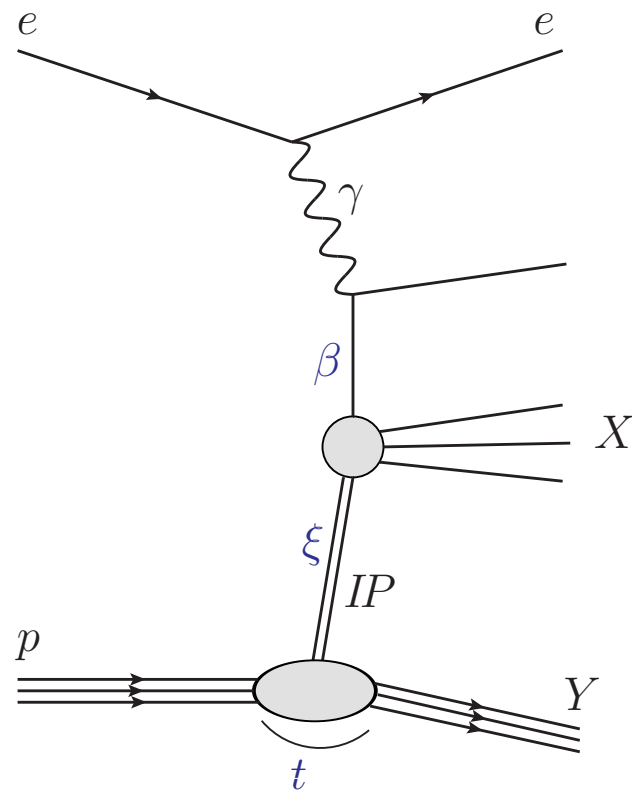
Ratio in saturation model: enhancement



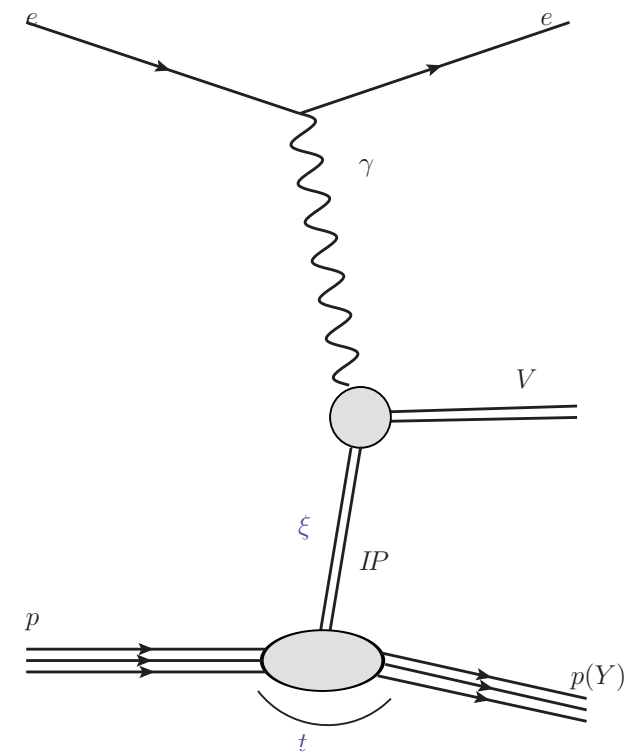
Yellow Report

Example : diffractive elastic vector meson production

Inclusive diffraction



Final state contains only vector meson, scattered lepton and proton



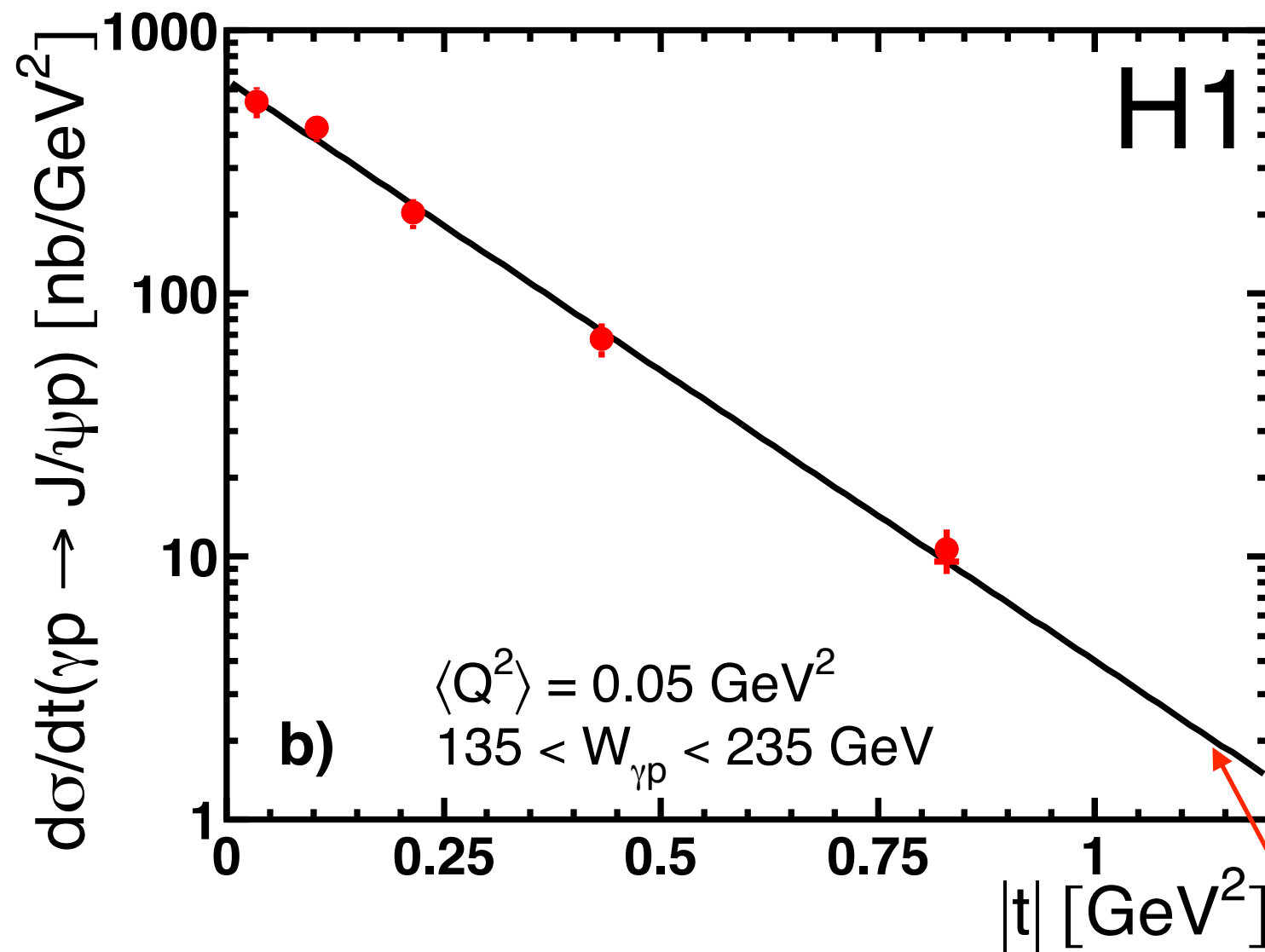
J/ ψ vector meson: charm -anti charm system

$$m = 3.09 \text{ GeV}$$

Upsilon vector meson: bottom - anti bottom system

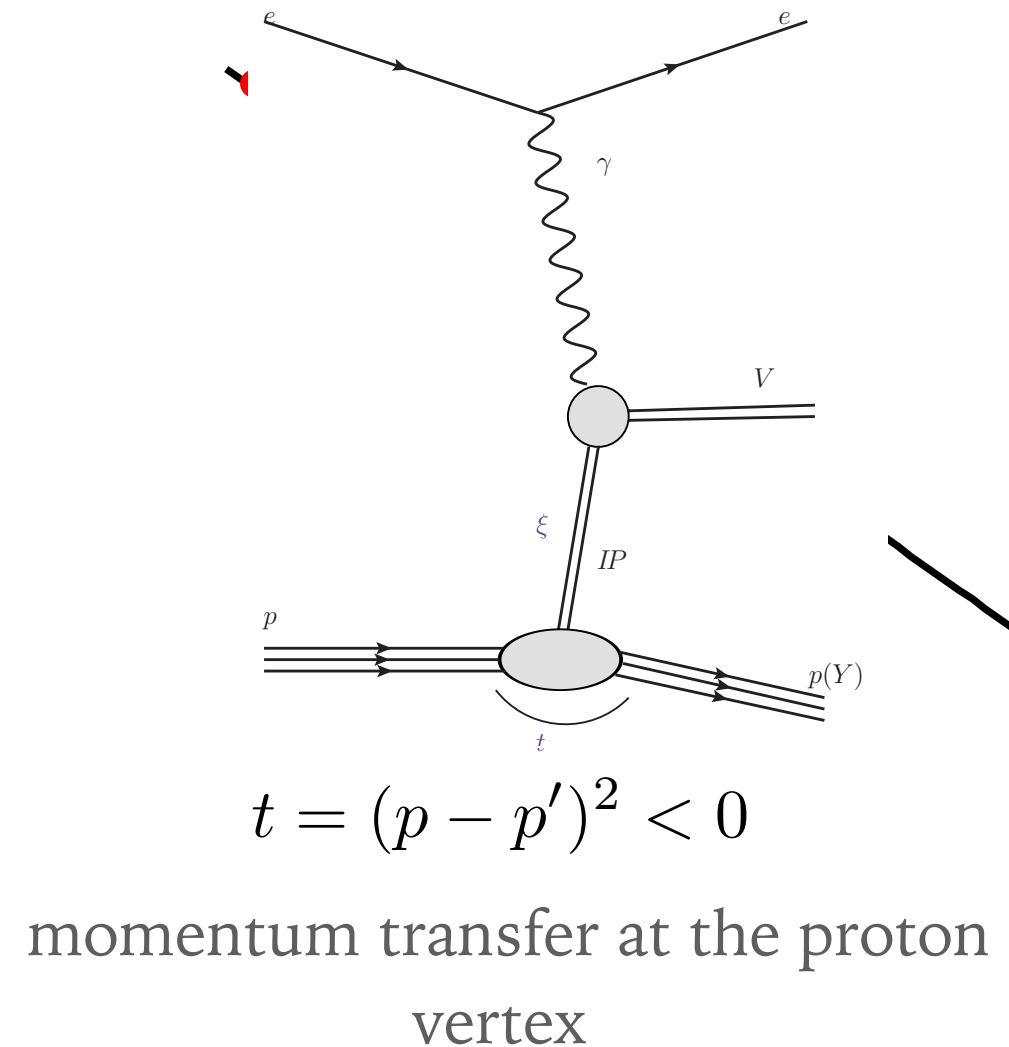
$$m = 9.46 \text{ GeV}$$

Elastic vector meson production



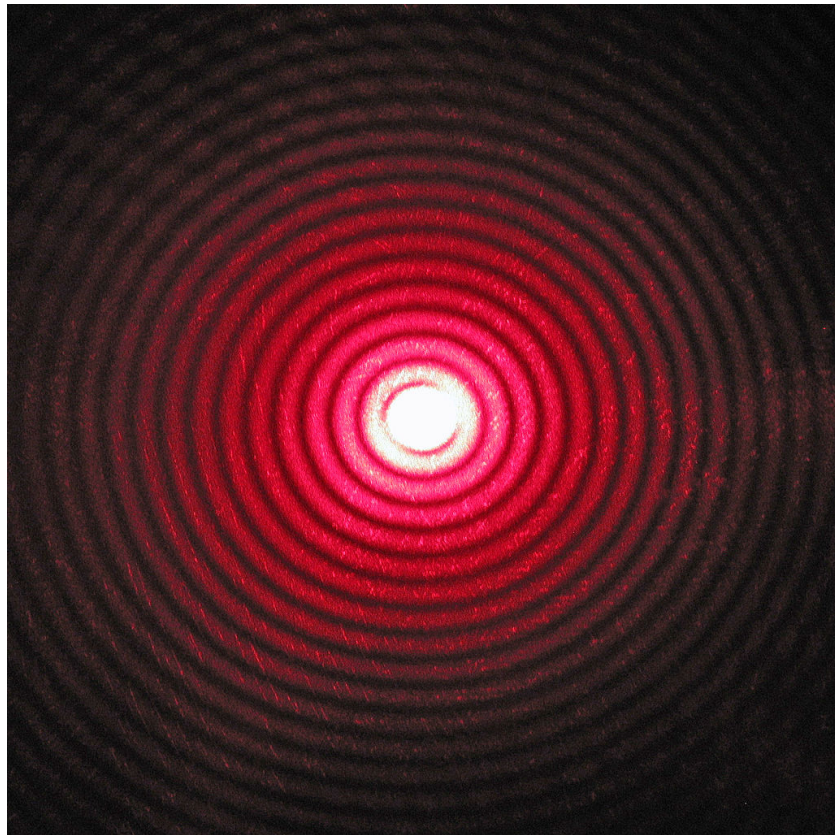
$$\frac{d\sigma}{dt} \sim e^{bt}$$

Exponential fit



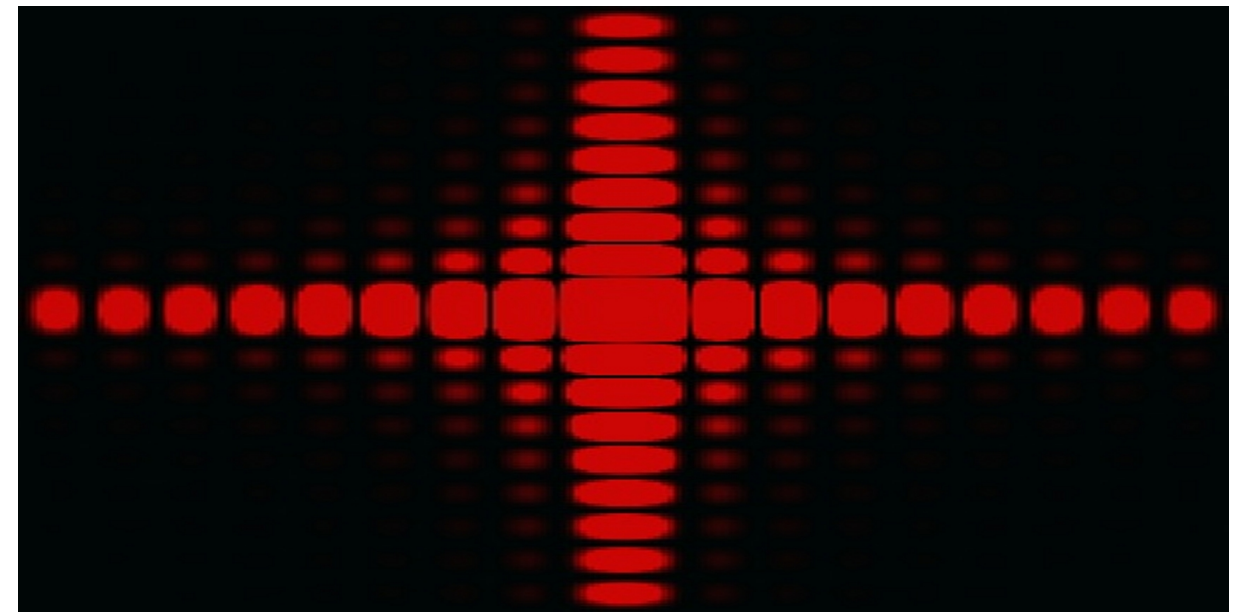
t-dependence of the elastic cross section provides information about the profile of the target

Diffraction in hadronic physics: analogy with optics



Source: Wikipedia
Author: Wisky

Circular aperture



Source: Wikipedia
Author: Epzcaw

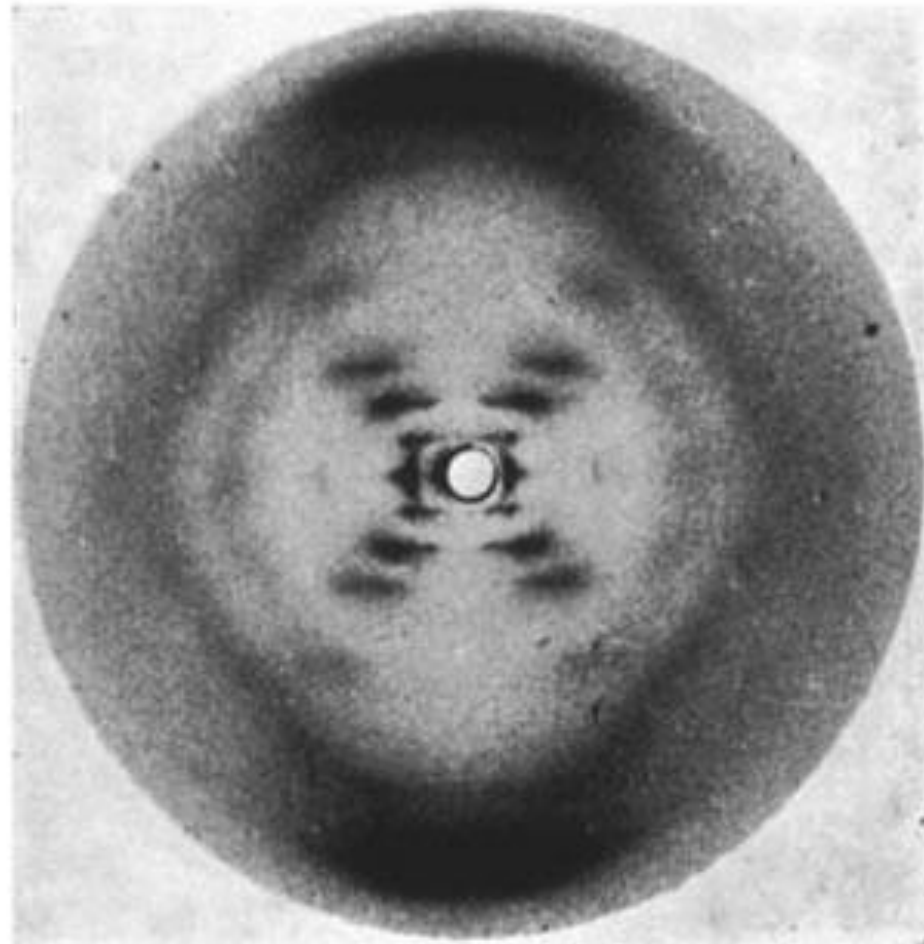
Rectangular aperture

The diffraction pattern (far away from obstacle) is a Fourier transform of the apertured field.

Diffraction pattern

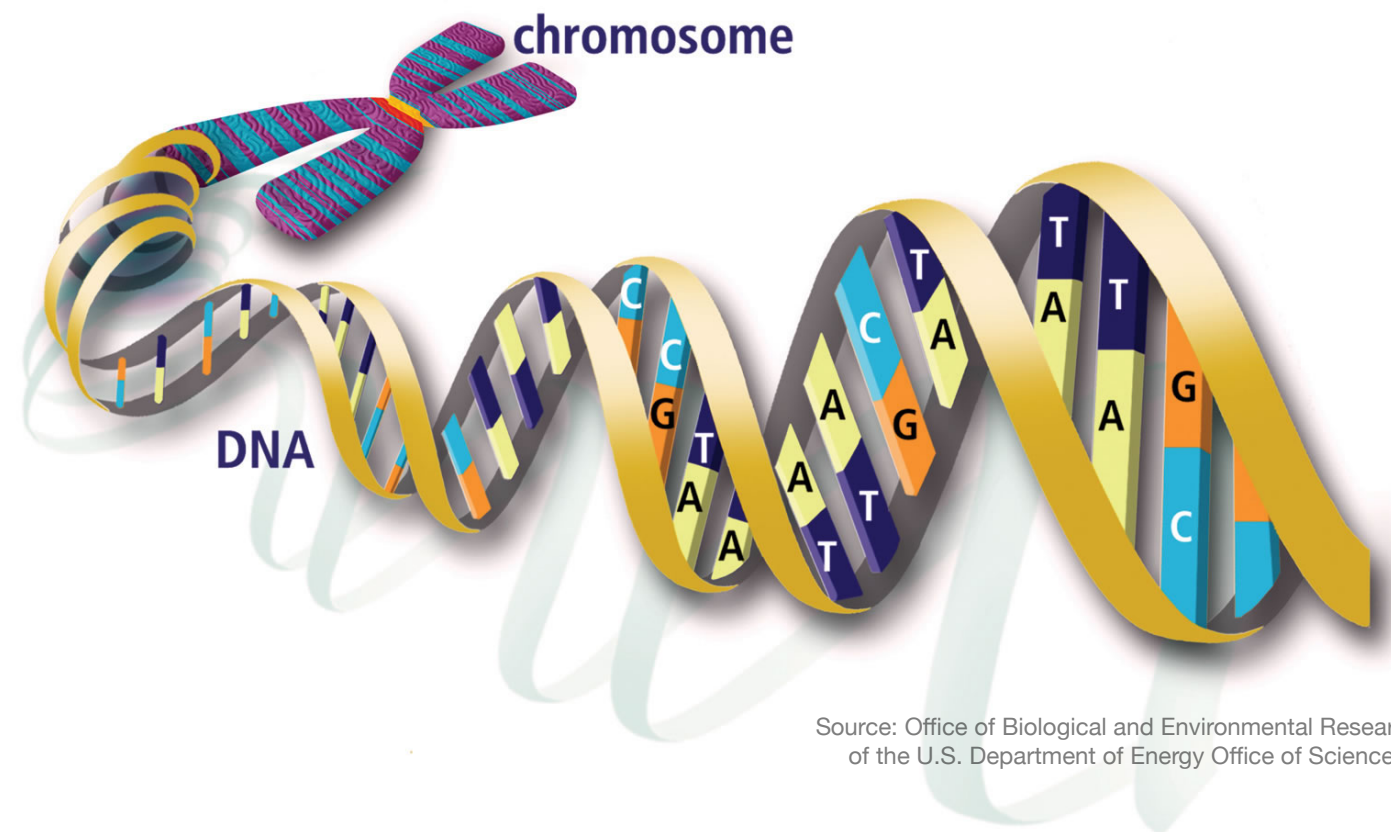
Photo 51

Gosling-Franklin



Source: Wikipedia

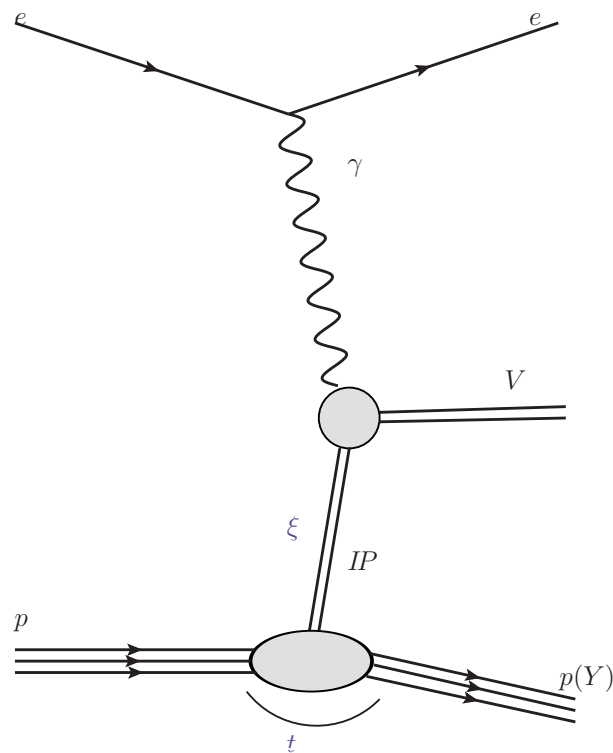
Watson-Crick



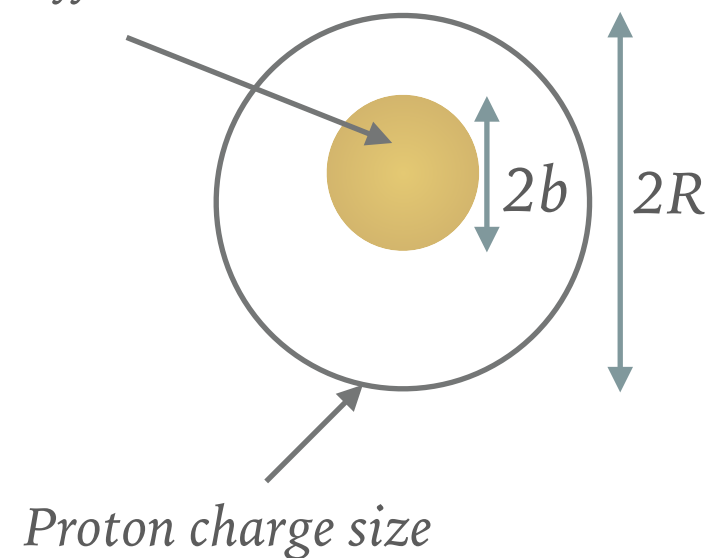
Diffraction can provide very detailed information about the structure of an object. The object cannot be destroyed in this process.

Diffractive elastic VM production

Diffractive elastic vector meson production as a way to study nucleon structure



Measured in diffractive VM



Radius measured in diffractive scattering of vector mesons

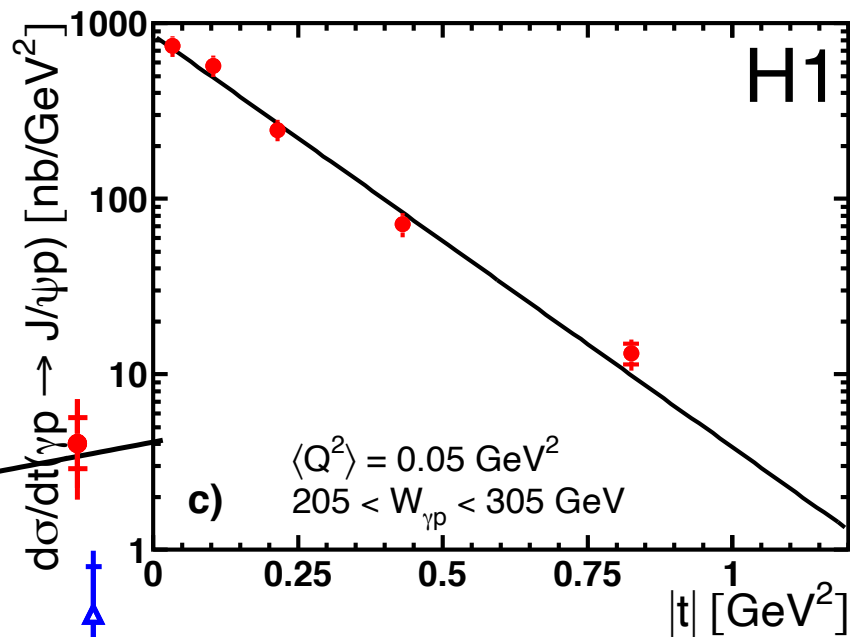
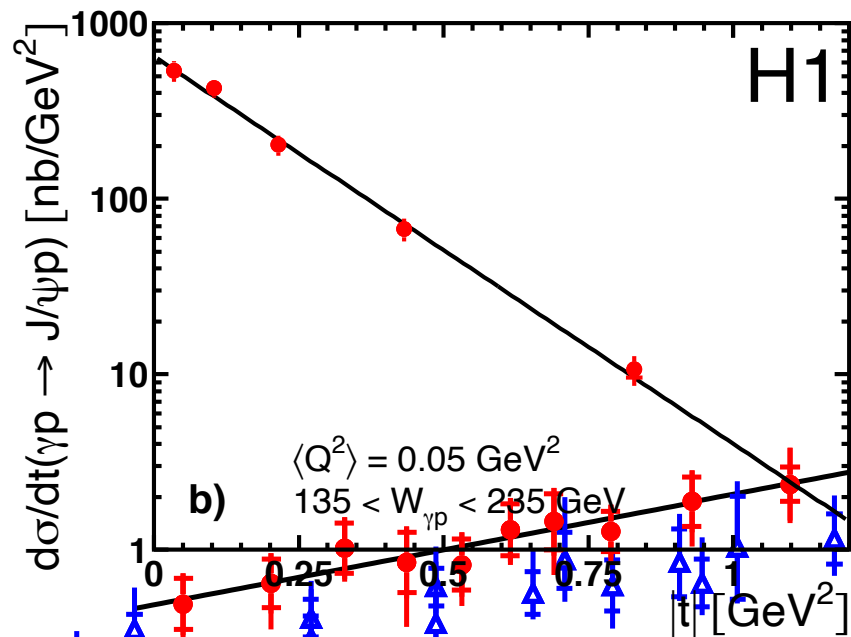
$$b \approx 0.5 \div 0.6 \text{ fm}$$

Proton charge radius

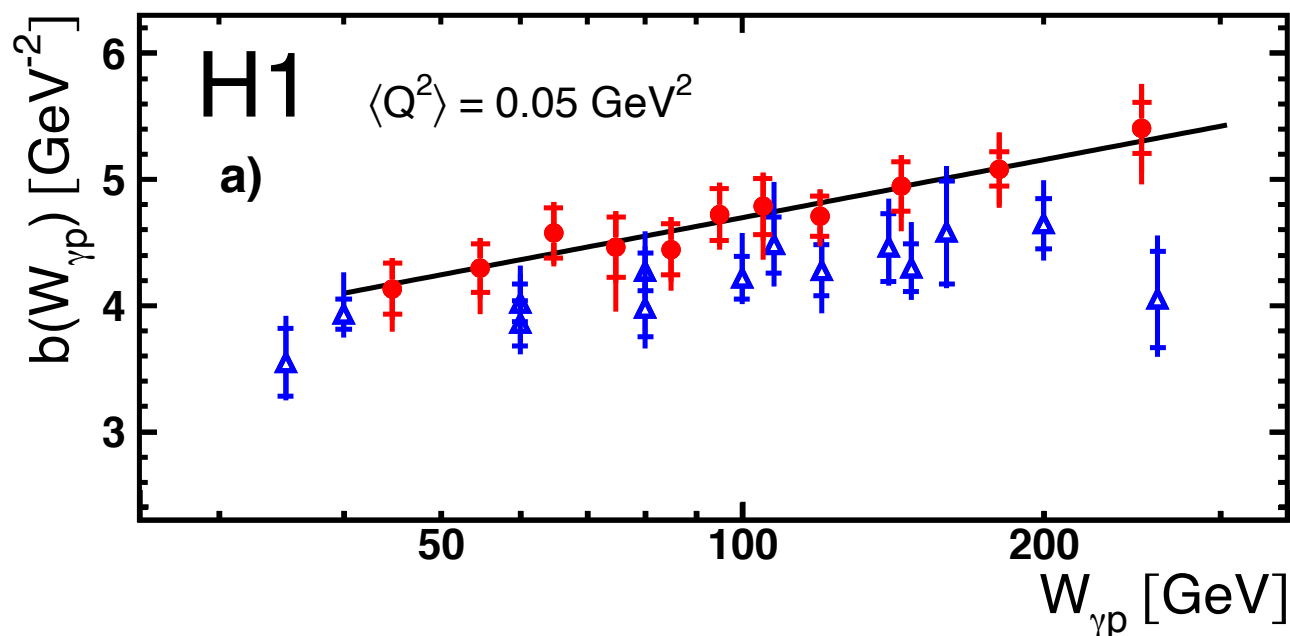
$$R \approx 0.84 \div 0.87 \text{ fm}$$

Experiments on elastic VM production suggest gluons are concentrated in smaller regions than quarks

Growth of the target size with energy



$$\frac{d\sigma}{dt} \sim e^{bt}$$

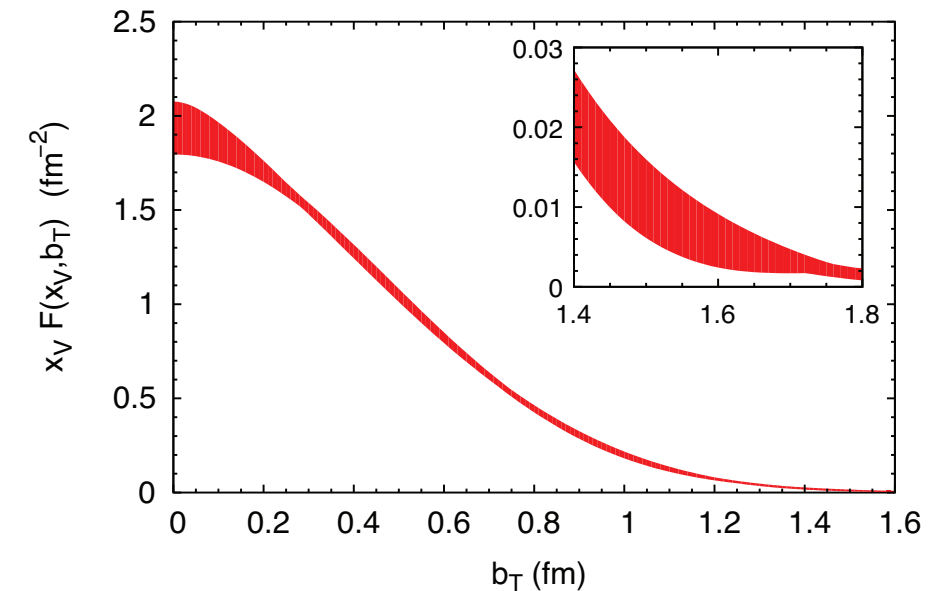
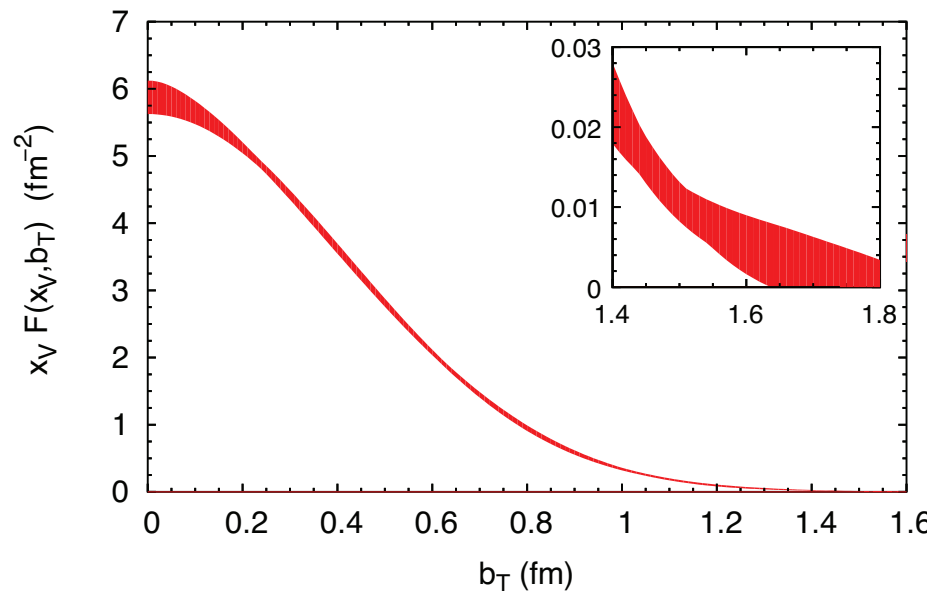
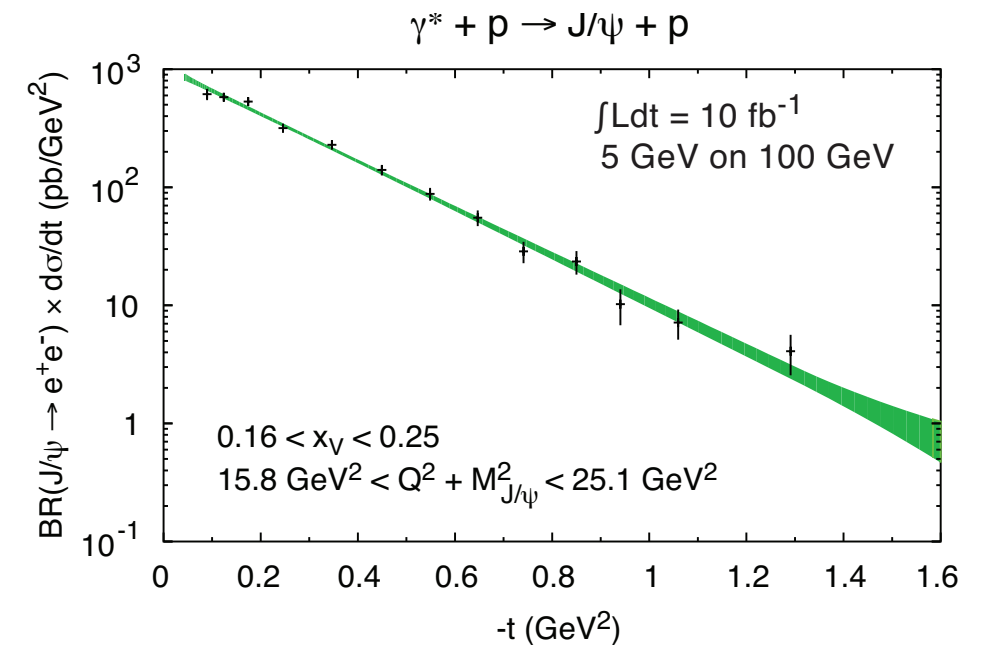
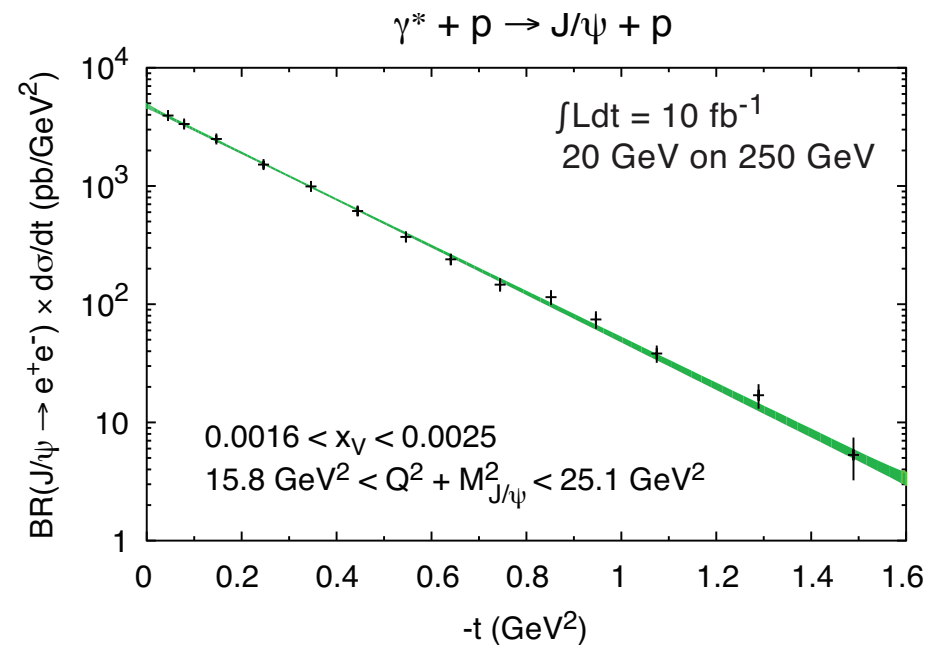


The slope grows with energy:

$$b(W) = b_0 + 4\alpha' \ln(W_{\gamma p}/W_0)$$

Elastic vector meson production at EIC

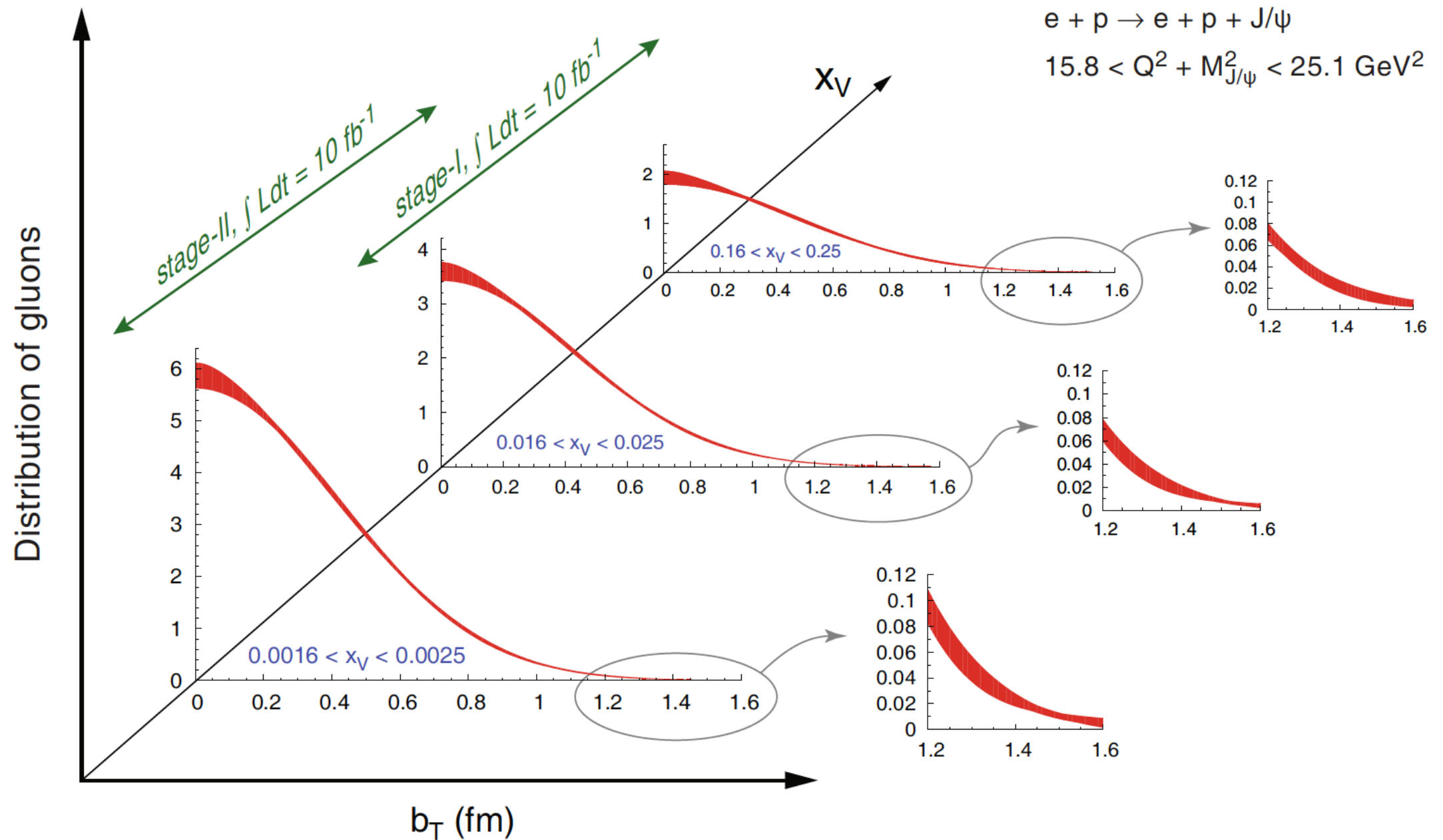
Fourier transform



EIC, White paper

EIC: lower energy than HERA, different kinematics.
Very high statistics, high precision

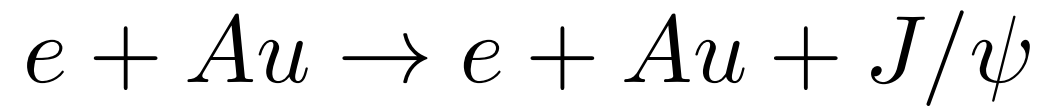
Profile function from elastic vector meson production



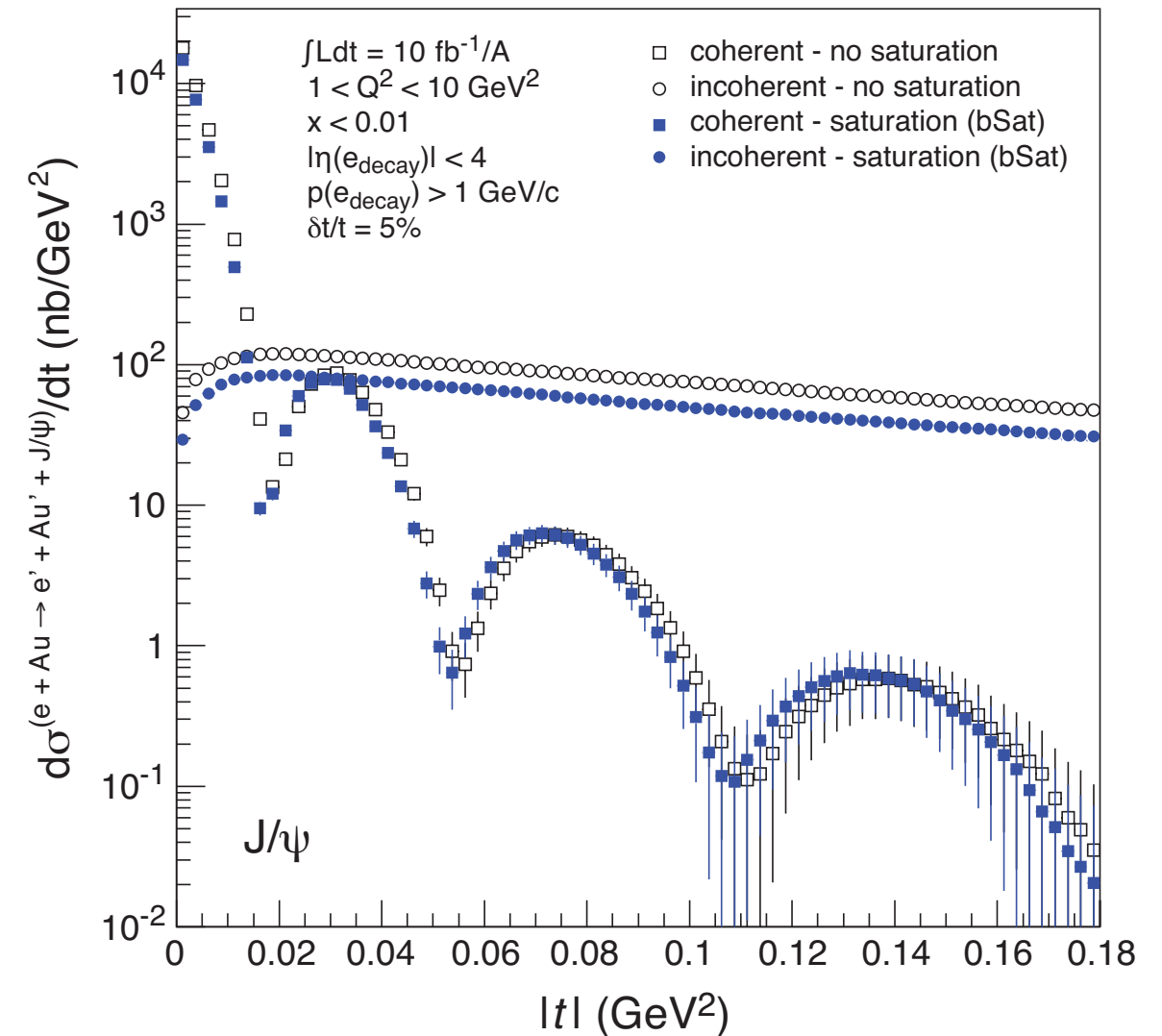
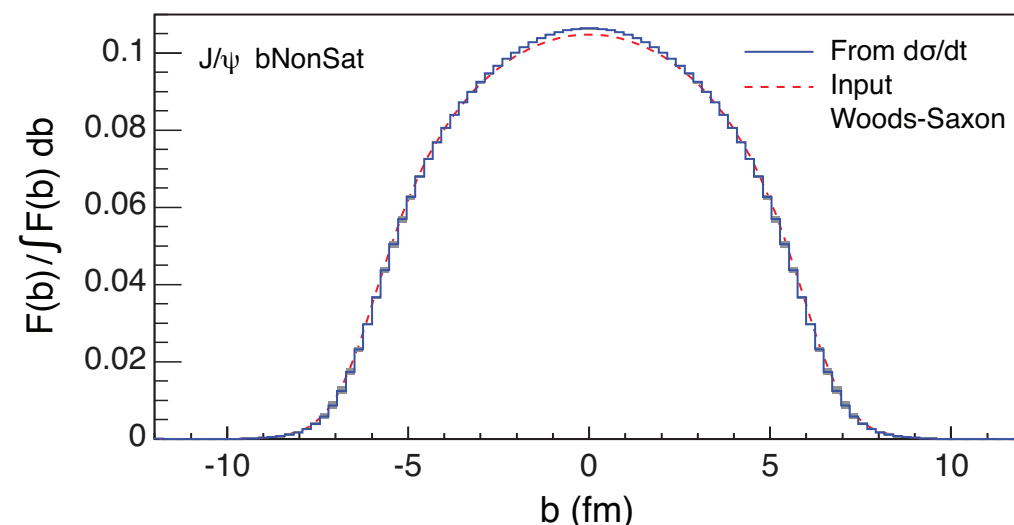
Elastic vector meson production at EIC : eA

EIC, White paper

Nuclear target: Au



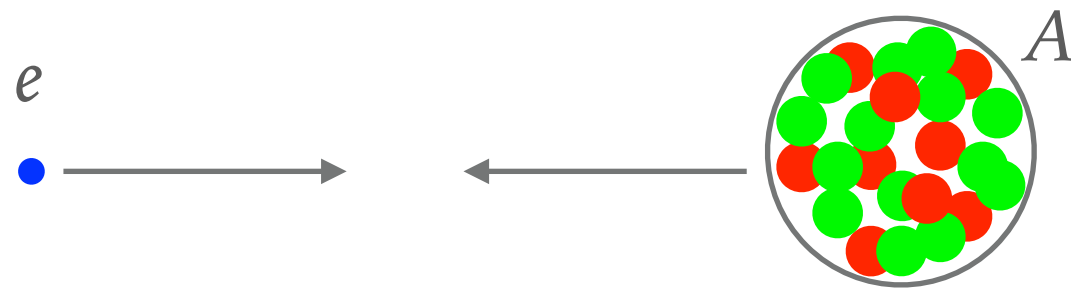
Characteristic 'dips' in t-distribution



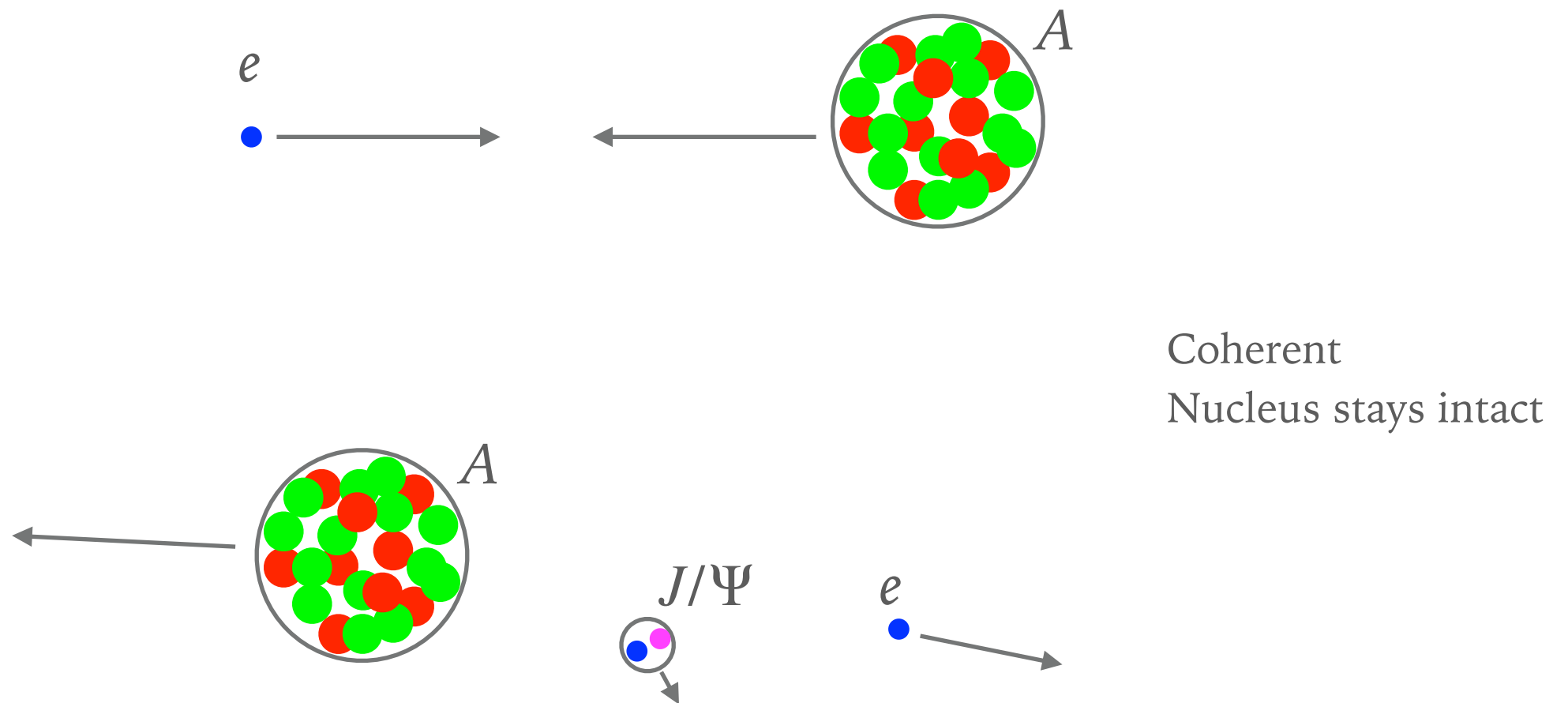
$$F(b) = \int_0^\infty \frac{q dq}{2\pi} J_0(qb) \sqrt{\frac{d\sigma_{\text{coherent}}}{dt}}$$

$$t = -q^2$$

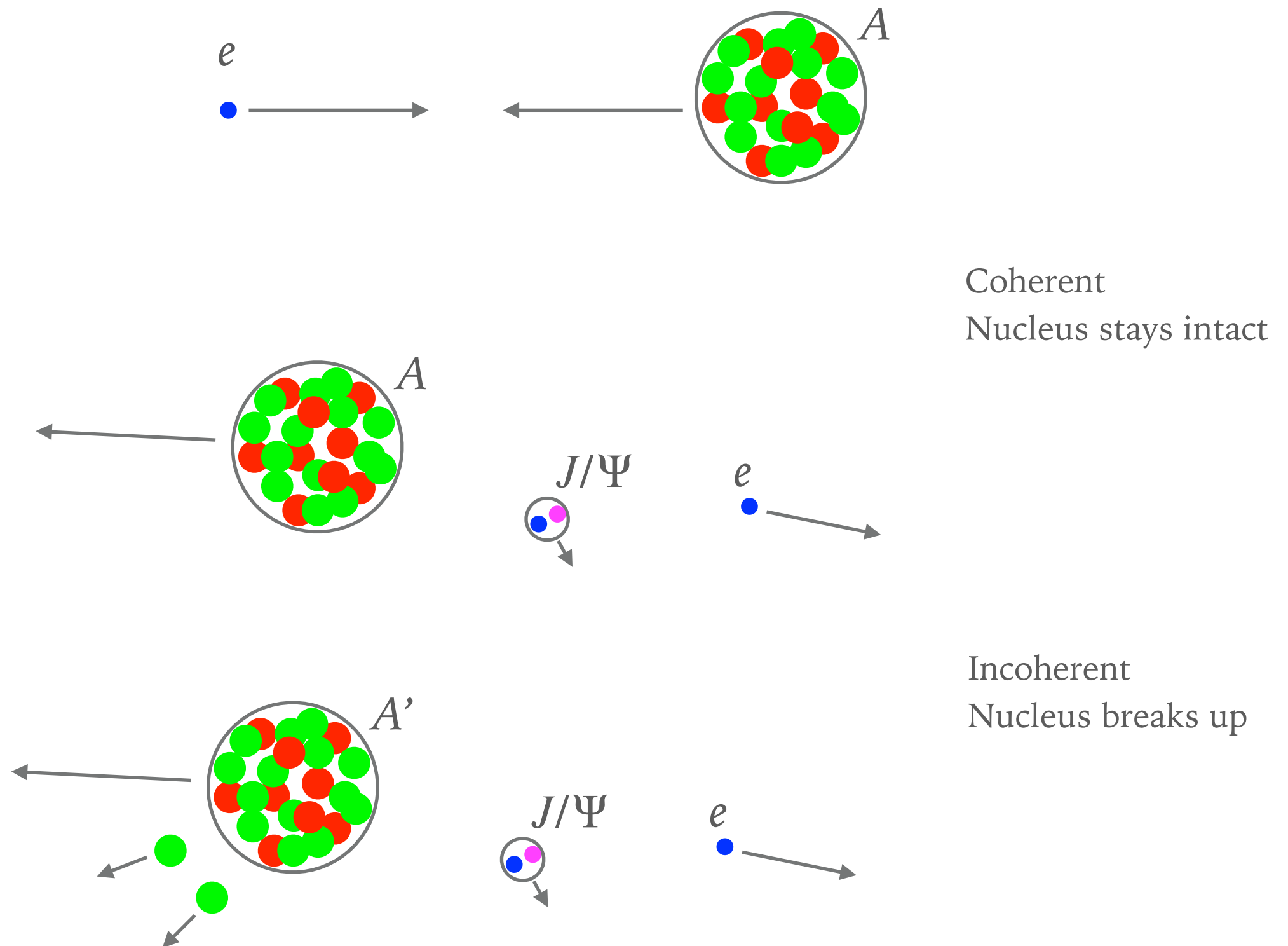
Coherent vs incoherent



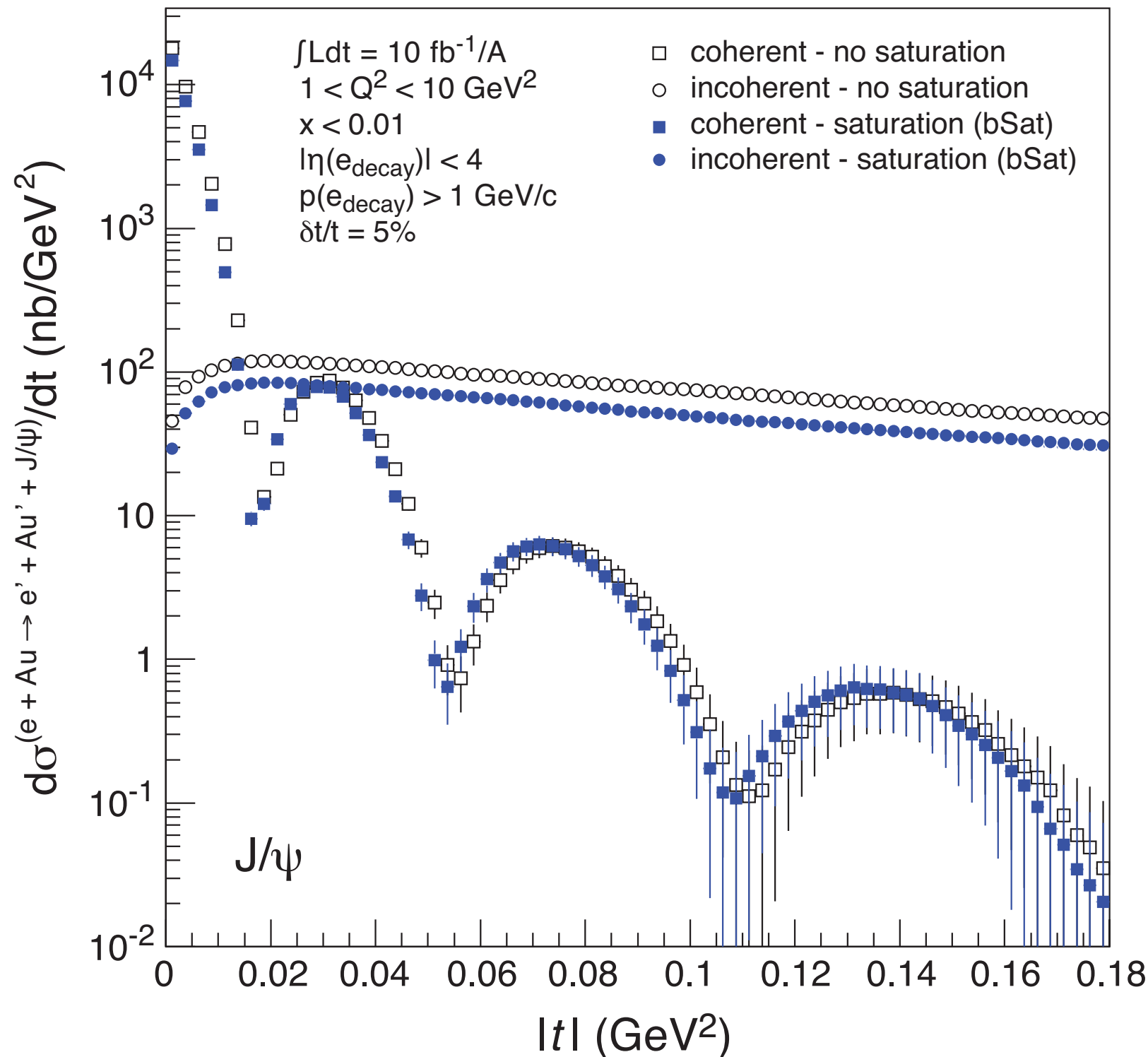
Coherent vs incoherent



Coherent vs incoherent



Coherent vs incoherent



Coherent:

Depends on the shape of the source, average distribution

Incoherent:

Provides information about the fluctuations or lumpiness of the source

Physics at small x and with nuclei at EIC

- **Nuclear structure functions**, precision extraction of nuclear PDFs, testing the **limits** of **collinear factorization** in nuclei. Initial conditions for hot QCD.
- Explore the onset of **saturation** in **eA**, DGLAP vs non-linear evolution, x, A , and Q dependence. Precise measurement of F_L needed (variable energies)
- Extraction of **diffractive nuclear PDFs** possible for the first time, potential for F_L^D . Prospects for measuring Reggeon. **Diffractive to inclusive ratios** needed to distinguish between the different scenarios (saturation vs leading twist shadowing).
- **Exclusive** diffraction of vector mesons, excellent process to **map spatial distribution** and test **saturation**. Experimental challenges.